Light Transmittance through PEG1500 during Crystallization

# Detecting State of Charge in PCMs
Experimental investigation of changes in chemical and physical properties during phase transitions

Master's thesis in the Master's Programme Innovative and Sustainable Chemical Engineering

ROBERT PABERIT
JOHAN ÖJERBORN

# Detecting State of Charge in PCMs

Experimental investigation of changes in chemical and physical properties during phase transitions

*Master's Thesis in the Master's Programme Innovative and Sustainable Chemical Engineering*

ROBERT PABERIT

JOHAN ÖJERBORN

Detecting State of Charge in PCMs
Experimental investigation of changes in chemical and physical properties during
phase transitions

*Master's Thesis in the Master's Programme Innovative and Sustainable Chemical Engineering*

ROBERT PABERIT
JOHAN ÖJERBORN

Department of Civil and Environmental Engineering
Division of Building Technology
Chalmers University of Technology
SE-412 96 Göteborg
Sweden
Telephone: +46 (0)31-772 1000

Cover:
Picture taken from section 5.4 and shows how the light transmittance through
PEG1500 changes during crystallization.

Detecting State of Charge in PCMs
Experimental investigation of changes in chemical and physical properties during
phase transitions

*Master's Thesis in the Master's Programme Innovative and Sustainable Chemical
Engineering*

ROBERT PABERIT
JOHAN ÖJERBORN
Department of Civil and Environmental Engineering
Division of Building Technology
Chalmers University of Technology

# Abstract

The energy use in the residential sector has steadily increased during the last decades as a consequence of an increased demand for heating and cooling in buildings. One of the main problems when it comes to indoor climate control is that the energy is not used efficiently. For instance, energy is used to heat the building during cold nights and additional energy is used to cool the building during hot days. Ideally the excess energy generated during the day could be stored and then released into the building during the night, thus reducing the energy use and energy losses. This effect could be realized utilizing the potential of phase change materials (PCMs). A PCM is a material that is able to store and release large amounts of energy with respect to its volume through solid-liquid phase transitions. By introducing PCMs in building envelopes it is possible to reduce the energy demands for indoor climate control in the building up to 25 %. To facilitate implementation of PCM solutions in buildings it is important to be able to visualize that the material is active. This can be done by measuring the proportions of the material that is either in liquid or solid state, also called the state of charge (SOC) at any given time.

The main purpose of this master's thesis is to investigate non-destructive and quantitative methods to measure the SOC in order to support implementation of technical PCM solutions in the future. It is also important that the methods can be commercially suitable when it comes to economic, environmental and technical aspects. This has been done utilizing the fact that the physical, chemical and thermal properties of a material changes during phase transitions and could possibly be correlated to the SOC. Based on the results presented in this study, changes of certain properties correlate better to the SOC than others depending on the investigated PCM type (polymers, sugar alcohols and salt hydrates). The change in light transmittance as a PCM undergoes phase transition has seen to correlate well to the SOC for all of the investigated PCM types, additionally this method shows good commercial and technical implementation potential.

**Keywords**: Phase change material (PCM); Phase transition; State of charge (SOC); Visualization; Thermal energy storage (TES); Latent heat (LH); Building application; Differential scanning calorimetry (DSC); Electrical resistance; Light Transmittance

Bestämning av laddningsgrad för fasövergångsmaterial
Experimentell undersökning av förändringar av kemiska och fysiska egenskaper
under fasövergångar

*Examensarbete inom mastersprogrammet innovativ och hållbar kemiteknik*

ROBERT PABERIT
JOHAN ÖJERBORN
Institutionen för bygg- och miljöteknik
Avdelningen för byggnadsteknik
Chalmers tekniska högskola

# Sammanfattning

Energianvändningen i bostadssektorn har ökat stadigt de senaste decennierna i takt med ett ökat behov av uppvärmning och kylning av byggnader. Ett av huvudproblemen vid temperaturreglering av inomhusklimatet är att energin inte används effektivt. Exempelvis används energi både för uppvärmning under kalla nätter och ytterligare energi används för kylning under varma dagar. Det optimala vore att lagra den överskottsenergi som finns tillgängliga under dagen för att sedan använda den för uppvärmning under natten. På detta sätt minskar både energianvändandet och energiförlusterna. Denna effekt kan förverkligas genom att utnyttja potentialen hos fasövergångsmaterial (PCM). PCM är material som kan lagra och frigöra stora mängder energi i förhållande till sin volym genom fasövergångar mellan fast och flytande form. Genom att introducera PCM i byggnader är det möjligt att reducera energianvändningen för temperaturreglering av inomhusklimatet med upp till 25 %. För att underlätta implementering av PCM-lösningar i byggnader är det viktigt att kunna visualisera att materialet är aktivt. Detta kan göras genom att mäta hur stora proportioner av materialet som är i antingen fast eller flytande form, även kallat laddningsgrad (SOC) vid en given tidpunkt.

Huvudsyftet med detta examensarbete är att undersöka icke-destruktiva och kvantitativa metoder för bestämning av SOC för att underlätta implementering av tekniska PCM-lösningar i framtiden. Det är också viktigt att metoderna är kommersiellt tillämpbara ur ekonomisk, miljömässig och teknisk synvinkel. Detta har gjorts genom att dra nytta av att fysiska, kemiska och termodynamiska egenskaper i materialet förändras under fasövergångar och kan potentiellt vara kopplade till SOC. Resultaten från denna studie visar att förändringen av vissa egenskaper har en tydligare koppling till SOC än andra, beroende på vilken typ av undersökt PCM som använts (polymerer, sockeralkoholer och salthydrater). Förändringen av ljusgenomsläpp då materialet genomgår en fasövergång kan kopplas till SOC för alla de undersökta PCM-typerna, dessutom visar denna metod god teknisk och kommersiell tillämningspotential.

**Nyckelord**: Fasövergångsmaterial (PCM); Fasövergång; Laddningsgrad (SOC); Visualisering; Termisk energilagring (TES); Latent värme (LH); Byggtillämpningar; Differentiell svepkalorimetri (DSC); Elektrisk resistans; Ljusgenomsläpp

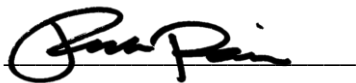# Contents

# Preface by the Authors

This Master's thesis aimed to develop and evaluate new ways to determine the state of charge in different PCMs. It was performed at the department of Civil and Environmental Engineering, Chalmers University of Technology between January and June 2016. The supervisors during this thesis has been Helén Jansson, associate Professor, Civil and Environmental Engineering at Chalmers University of Technology and Pär Johansson, assistant Professor, Civil and Environmental Engineering at Chalmers University of Technology where the first mentioned also was the examiner.

First and foremost, we want to thank our supervisors Helén Jansson and Pär Johansson for their support and guidance throughout this project.

The experimental part of this master's thesis would not have been doable without the following people which we thank gratefully;

- Marek Machowski, Mattias Zetterberg, Mona Pålsson and Håkan Larsson: for lending us measurement equipment
- Jan Swenson, Khalid Elamin, Christoffer Olsson and Lars Hellberg: for opening up their laboratory for us at the Physics department
- Pepe Tan: for providing us with materials for testing

Last but not least we want to express our gratitude and appreciation to our opponents, Mia Höök and Linus Ögren for their valuable and constructive suggestions during the final completion of this thesis.


Robert Paberit                                    Johan Öjerborn

# List of Figures

# Abbreviations

| | | |
|---|---|---|
| DHFMA | - | Dynamic heat flow meter apparatus |
| DSC | - | Differential scanning calorimetry |
| HFMA | - | Heat flow meter apparatus |
| LH | - | Latent heat |
| PCM | - | Phase change material |
| PEG | - | Polyethylene glycol |
| SOC | - | State-of-charge |
| TES | - | Thermal energy storage |
| TPS | - | Transient plane source |

| | | |
|---|---|---|
| $C_{eff}$ | - | Effective volumetric heat capacity, $[kJ/m^3K]$ |
| $c_P$ | - | Specific heat capacity, constant pressure, $[kJ/kgK]$ |
| $c_{reference}$ | - | Specific heat capacity of the reference, $[kJ/kgK]$ |
| $c_{sample}$ | - | Specific heat capacity of the sample, $[kJ/kgK]$ |
| $E$ | - | Electric field, $[V/m]$ |
| $\Delta G$ | - | Change of Gibbs free energy, $[kJ/kg]$ |
| $H$ | - | Enthalpy, $[kJ/kg]$ |
| $\Delta H_c$ | - | Enthalpy of crystallization, $[kJ/kg]$ |
| $\Delta H_m$ | - | Enthalpy of melting, $[kJ/kg]$ |
| $I$ | - | Current, [A] |
| $J$ | - | Current Density, $[A/m^2]$ |
| $L$ | - | Sample thickness, [m] |
| $Q$ | - | Heat flow, $[W]$ |
| $\dot{Q}$ | - | Heat flux, $[W/m^2]$ |
| $r$ | - | Specific thermal resistance, $[Km^2/W]$ |
| $R$ | - | Resistance, $[\Omega]$ |
| $s$ | - | Calibration factor, [-] |
| $\Delta S$ | - | Entropy change, $[kJ/kgK]$ |
| $T_{ambient}$ | - | Ambient temperature, [°C] |
| $T_c$ | - | Crystallization temperature, [°C] |
| $T_m$ | - | Melting temperature, [°C] |
| $T_{reference}$ | - | Reference temperature, [°C] |
| $T_{sample}$ | - | Sample temperature, [°C] |
| $\Delta T$ | - | Temperature difference, [°C] |
| $\Delta T_{sub}$ | - | Subcooling, [°C] |
| $U$ | - | Voltage, [V] |

| | | |
|---|---|---|
| $\sigma$ | - | Conductivity, $[S/m]$ |
| $\tau$ | - | Time interval, $[s]$ |

# 1. Introduction

The energy use in the residential and commercial sectors has steadily increased since the 1980's and is now representing approximately 35 % of the total energy usage in the world (1). This sectorial trend of increased energy usage is not expected to drop, but rather to increase even more in the future, and one of the most important factors contributing to this development is the increased demands for heating and cooling in buildings (2). In order to reduce the need for heating in buildings and minimize the heat loss, more advanced and complex insulation materials are introduced on the market each year (3).

Another problem is that the accessibility and demand for energy in buildings does not always conform. For instance, energy may be needed to heat up a building during a cold night and then more energy is needed to cool the building as the outdoor temperature increases during the day. This use of energy for both heating and cooling is not efficient. Ideally the excess solar radiation energy generated during the day could be stored and then released into the building during the night, thus preventing unnecessary energy use and energy loss. By introducing phase change material (PCM) in the envelope of a building, this effect could be realized. A PCM is a material that can store and release large amounts of energy through phase transitions in relation to its volume (commonly transitions between liquid and solid state). The material must be able to store and release energy reversibly throughout many cycles (over 10 000 cycles) without losing its energy storage potential. Thermal energy is stored in the material as the material melts into liquid state, it can then be released again (at a lower temperature) as the material crystallizes into a solid. This form of thermal energy storage (TES) can then be repeated again and again, making it possible to use PCM as an energy storage material throughout multiple day cycles. Recent studies has shown that the energy use for heating, cooling and air conditioning of buildings can be reduced up to 25 % by introducing PCMs in the structure (4).

In contrast to conventional sensible energy storage materials such as masonry, rock or water, PCMs are able to store 5-14 times as much energy per unit volume in their phase change temperature region. This is due to their large latent heat (LH) storage potential. As a PCM melts it is able to store a certain amount of energy without resulting in an increasing in temperature of the material (known as latent heat). This energy is called the melting enthalpy and is in theory equivalent to the energy released when the PCM crystallizes, called the crystallization enthalpy, which also occurs at constant temperature (5). There are many different types of commercially available PCMs, each with their own specific properties when it comes to heat storage capacity, phase transition temperature intervals, degree of subcooling (the difference between the melting and crystallization temperature), crystalline structure and other physical- and chemical properties (3).

To successfully implement PCMs in buildings it is important to verify its function by measuring the amount of energy stored in the material, or the state of charge (SOC) at a given time. This can easily be carried out when the material is either in completely liquid or completely solid state, but since phase transitions occur more or less isothermally it is not possible to use this technique during the actual melting

or crystallization. To be able to measure the SOC during the latent phase transition it is crucial to be able to determine the ratio of how much of the material that is in either solid or liquid state. As of today there are no reliable commercial method available to perform these kind of measurements (6). However, studies have been made trying to correlate volumetric change and damping properties to the SOC during phase transitions (7). This study aims to further investigate and test different kinds of analytical measuring techniques in order to either directly or indirectly be able to measure the SOC for different types of PCMs during latent phase transitions.

## 1.1. Background

The potential energy savings for indoor heating and cooling is estimated to be 11-25 % with PCMs integrated in building envelopes (4; 8). However, to fully exploit the potential of the PCMs, the occupants need good practical understanding and knowledge on how these user-adaptive envelopes perform. Technologies for visualizing the PCM activation process can increase the understanding and knowledge among the occupants and provide a larger chance for a successful implementation of PCM systems. However, today there is a pedagogical problem to explain how and when PCMs are active in regard to passive adjustment to changes of the environment. The reason for this is the lack of proper tools. Therefore, new and innovative analytical techniques and solutions to visualize the SOC are needed (6).

As a PCM undergoes a phase transition, the chemical and physical properties like thermal and electrical conductivities, thermal heat capacity, thermal diffusivity, density, viscosity, volume and different optical properties such as light transmittance and refractive index etc. are changed. These can be measured by different analytical methods. Different types of PCMs may have different property changes and with varying proportions. For instance, PCMs that are based on paraffins will have a larger volume change compared to PCMs based on inorganic materials (7). Therefore, there is a need for investigating different types of PCMs and to identify the most appropriate performance indicator for each PCM (salt hydrates, sugar alcohols, polymers etc.). By measuring and visualizing the changes of these performance indicators during phase transitions it is possible to get a good estimation of the activity of a PCM, using simple means and without having to use complex or expensive technology (7). This will increase the chances for successful implementation of PCM in buildings as a commercial product as well as to contribute to a better general understanding of how the material works.

## 1.2. Purpose

The purpose of this Master's thesis was to find the most appropriate performance indicator for various types of PCMs. One particular point of interest was to find cheap and reliable measurement techniques to visualize the SOC, i.e. to distinguish between the solid and liquid states of the material. Except for a more fundamental understanding of the behavior of different PCMs, the results of this project has revealed suitable performance indicators for specific types of PCMs. This will facilitate implementation of PCMs as energy storage materials in buildings in the near future, making it a new and sustainable way to save energy.

## 1.3. Limitations

With respect to the application of the PCMs as energy storage materials in buildings, the PCMs must have transition temperatures within the range of common indoor temperatures. This restriction limited the investigated PCMs to polymers, paraffins, salt hydrates and possibly sugar alcohols. All of these PCM types has been investigated in this study except for paraffins due to limited availability (at the department) of the material. The experiments will be conducted on a macroscopic level with the ambition to verify and visualize the function of the PCMs by utilizing the property changes occurring during phase transitions. Finding nondestructive measuring techniques has been of primary focus, as well as investigating whether or not it is possible to implement the techniques in commercial applications.

## 1.4. Objective

The main objectives of this master's thesis was to find reliable and possibly commercially suitable analytical measurement techniques that either directly or indirectly measures or visualizes the activity of different types of PCMs. This can be summarized in the following research questions:

1. What are the most suitable performance indicators to visualize the SOC in PCMs based on polymers, sugar alcohols and salt hydrates?

2. How could the performance indicator(s) be implemented effectively to visualize the SOC in the PCM for a large scale building application?

# 2. Phase Changes – Concepts and Main Definitions

## 2.1. Phase Transitions

As a material absorbs energy from the surroundings, the internal energy of the molecules increases, resulting in a temperature rise. At a certain temperature the molecules have enough energy to initiate a phase transition. At this point all the energy absorbed is used to induce a phase transition instead of raising the temperature (i.e. isothermally). The energy needed to induce a phase transition from solid to liquid is called the melting enthalpy, ($\Delta H_m$). In the same manner, a phase transition from liquid to solid is also isothermal, the difference being that energy instead is released during the phase transition. This amount of energy is called the crystallization enthalpy, ($\Delta H_c$), and is in theory equivalent to the melting enthalpy (9). Figure 1 illustrates how the temperature of a material changes with increased amount of absorbed energy in the region of melting. As the amount of absorbed energy increases the temperature of the material increases linearly until it reaches its melting temperature (sensible region, first segment in figure 1). At this temperature, additional absorbed energy does not result in an increased temperature of the material (isothermal conditions) but is used to induce a phase transition from solid to liquid (latent region, second segment in figure 1). The total amount of energy needed to complete this phase transition is equivalent to the melting enthalpy of the material. As the phase transition is complete, additional absorbed energy will once again result in an increase in temperature of the material (sensible region, third segment in figure 1).
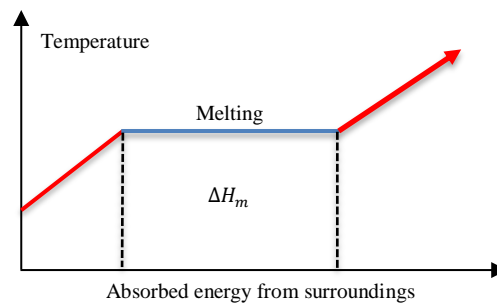


*Figure 1: This figure shows the temperature behavior in a material as the amount of absorbed energy increases. The heat storage can be considered both sensible (the regions before and after the melting) and latent (the isothermal melting region).*

According to Gibbs function of state, a system is assumed to be in equilibrium if the difference in free energy ($\Delta G$) is zero. During phase transition i.e. from solid to liquid, the system is in equilibrium, namely:

$$\Delta G_m = \Delta H_m - T\Delta S_m = 0 \qquad\qquad (i)$$

Where $\Delta H_m$ is the amount of energy required to induce a change in the system, in this case the melting enthalpy, $T$ is the temperature at which the phase transition

occurs and $\Delta S_m$ is the entropy change throughout the phase transition (9). For liquids, the change in enthalpy is thermodynamically expressed as:

$$\Delta H \approx \int_{T_1}^{T_2} c_p(T) dT + V\Delta P \qquad (ii)$$

Where $c_p$ is the specific heat capacity at constant pressure which is integrated over the temperature before and after heating or cooling ($T_1$ and $T_2$), $V$ is the volume of the system and $\Delta P$ is the pressure difference arising as the material changes from liquid to solid. In some cases the last term in this expression is neglected due to the relatively small changes in volume and pressure as a material changes between liquid and solid state (9).

## 2.2. Classification of Phase Change Materials

PCMs are often categorized as either organic (i.e. polymers, paraffins and sugar alcohols), inorganic (i.e. salt hydrates and metals) or eutectic materials (mixtures of two or more organic or inorganic materials). Each type of PCM has its own typical temperature and melting enthalpy region, seen in figure 2 (3; 10). Salt based PCMs are seen to operate in a high temperature region with a wide range of energy storage potential (melting enthalpy). In the opposite end, salt water mixtures have a narrower melting enthalpy interval and operates at low temperatures. PCMs that could be suitable for energy storage in buildings are found in between these types, namely; polymers/paraffins, salt hydrates and possibly sugar alcohols.
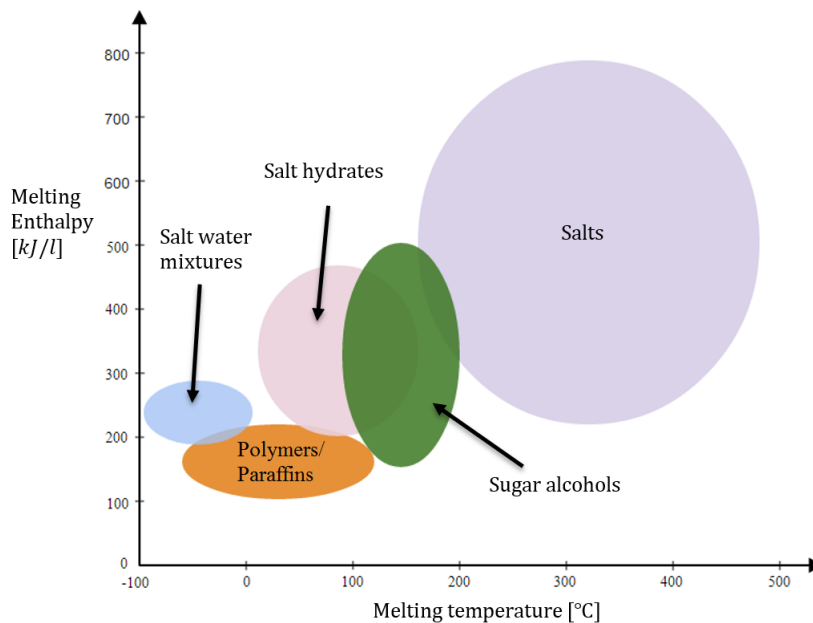


***Figure 2:*** *The figure shows the melting temperature and melting enthalpy for different types of PCMs. Recreated from Kalnæs, Jelle (3).*

### 2.2.1. Organic Compounds

Organic PCMs are generally divided into paraffins and non-paraffins. The paraffins show properties such as non-reactivity, non-corrosiveness, recyclability, chemical stability and good cohesive properties (5). Additionally, the paraffins do not separate during repeated cycles of melting and crystallization. The non-paraffins

(e.g. fatty acid and sugar alcohols) shows similar properties to the paraffins mentioned before (3). However, the paraffins undergoes relatively large volume change compared to the non-paraffins during phase transition (10). Furthermore, organic PCMs are often more expensive than inorganic PCMs, such as salt hydrates. Typical amount of thermal energy storage in organic polymeric PCMs are about $150 \pm 50 \ kJ/l$ (3).

### 2.2.2. Inorganic Compounds

Saltwater mixtures, metals and salt hydrates are examples of inorganic PCMs. However the only inorganic materials that are of interest for PCM applications in buildings are salt hydrates. Metals, in general, have really high melting temperatures and high density which makes them unsuitable for PCM solutions in buildings. The opposite problem is seen for salt water mixtures where the melting temperature is too low for the material to be utilized for building purposes. The salt hydrates are mixtures of inorganic salts and water which makes them highly available and cheap. In addition, salt hydrates have higher LH per unit mass, are non-flammable, have higher thermal conductivity and are generally cheaper than organic materials (3; 5). However, most of the salt hydrates are corrosive to most metals and can decompose during phase transitions due to release of bound water (10). Despite of this, the salt hydrates are still attractive to be used as PCMs due to their high thermal energy storage capacity, about $350 \pm 150 \ kJ/l$ (3).

### 2.2.3. Eutectic Mixtures

Eutectics are mixtures of two or more components that forms a minimum melting or crystallization temperature composition when being mixed in a specific ratio. When mixing multiple components they generally melt or crystallize separately at different temperatures. However for a eutectic mixture the different components coincides into one united melting or crystallization temperature that is lower than the melting or crystallization temperature of the ingoing components separately. One example of a eutectic mixture of lead and tin is to mix them in the ratio 62 % and 38 % respectively, resulting in a joint solidification temperature of 183 °C. This can be compared to the solidification temperatures of the pure materials which are 327 °C for lead and 232 °C for tin (11). This phenomena is illustrated in figure 3 where a eutectic mixture can be seen when mixing approximately 60 % of compound A with 40 % of compound B.
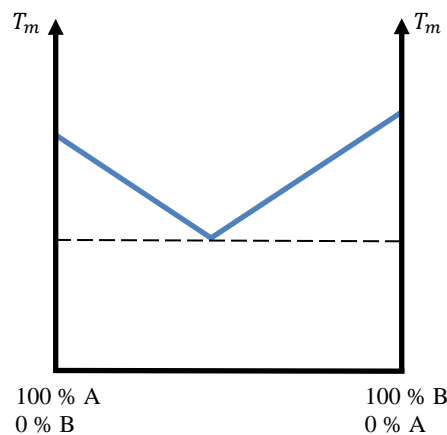


**Figure 3:** *This figure shows the typical behavior of eutectic mixtures which forms a minimum melting temperature composition when being mixed in a specific ratio.*

These PCMs often show distinct melting and crystallization points as the components undergoes simultaneous phase transition. Little research has been conducted on eutectic PCMs and the properties vary depending on the ingoing components (5). The thermal energy storage is marginally higher for eutectic mixtures than for the organic compounds. Typical transition temperatures for these mixtures are between 18-50 ℃ (10).

## 2.3.    Challenges with Different Phase Change Materials

Different types of materials shows different problematic features when it comes to their potential as PCMs. Sugar alcohols often suffer from severe degree of subcooling (sometimes up to 100 °C) and formation of amorphous metastable states during cooling (seen for e.g. xylitol which enters a highly viscous and transparent state instead of crystallizing). Subcooling is the difference between the melting and crystallization temperature and is illustrated in figure 4. These effects complicates their application as PCMs and makes them unsuitable to use in building applications (12).
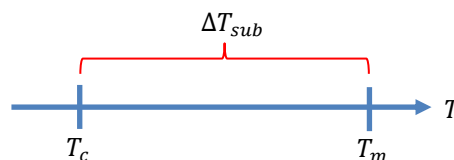


**Figure 4:** *This figure shows the temperature difference between the melting and crystallization temperature, also known as the subcooling.*

Even if the crystallization temperature may be in the range of normal indoor temperatures, the melting temperature is often much higher (i.e. seen for erythritol). This creates a problem as the material is never being exposed to temperatures high enough to melt and thus cannot store any latent energy. The ideal PCM for building applications should have a degree of subcooling that is less than the temperature difference between day- and nighttime. Experiments have been made trying to manipulate the melting and crystallization temperatures of sugar alcohols by adding urea. These experiments shows that a eutectic composition exists that reduces the melting temperature of erythritol. However, as a result the crystallization fails to occur at that composition (13).

Polymers and paraffins shows another problematic feature, namely low heat conductivity ($0.2\ W/mK$). This can be compared to the conductivity of commonly used building materials, such as cement boards or bricks, which have conductivities of $0.58\ W/mK$ and $0.72\ W/mK$ respectively (3; 14). This is problematic since the heat transfer between the active PCM and its surroundings is crucial for the function of the material. Ideally the PCM should have as high heat conductivity as possible, however to be considered good, the conductivity should be above $0.5\ W/mK$. Multiple studies have shown that it is possible to increase the thermal conductivity of polymers by introducing specific additives. Graphene, silver nanoparticles and β-aluminum nitride all increases the thermal conductivity of PEG, in some cases as much as to $1.7\ W/mK$ (15; 16; 17).

Salt hydrates have higher thermal conductivity in comparison to the organic materials (around $0.5\ W/mK$), however they suffer from chemical instability. Many salt hydrates releases bound water upon heating which may cause a change in the chemical composition of the material if not encapsulated hermetically. This can result in changes of the thermal properties such as transition temperatures and energy storage potential, thus affecting the use of the material (3).

## 2.4. Building Applications

PCMs can be applied in a number of different ways, either in porous construction materials or integrated in pipes or panels. However, for buildings the most appropriate applications are PCM-enhanced gypsum wallboards or PCM-enhanced concrete. The gypsum wallboards are cheap, commonly used in buildings and can be enhanced with several different PCMs. As the wallboards can be used throughout the whole building, it can provide possibilities for extensive thermal storage. The performance of the PCM-enhanced wallboards will depend on several factors such as the phase transition temperature, the LH storage capacity, the position of the wall, how the PCM are integrated in the wallboard etc. (3; 18). Concrete structural properties are already widely used in buildings today. By integrating PCM in the concrete you get so called thermocrete that will have both structural strength and thermostatic properties. There are different methods of how to contain the PCM within the concrete blocks; absorb it into the pores, absorb it into special silica cells or permeating it into polymeric carriers. These solutions gives an increased heat transfer area for the PCM compared to solutions where it is integrated in panels or pipes (18).

To prevent leakage and problems with expansion during the phase transition the PCMs needs to be contained in special containers. The containment of the material can be made either on micro or macro scale seen in figure 5. In micro scale, the PCM is integrated into the pores of a porous carrier material, such as wallboard or concrete, whereas in macro scale, the PCM alone is contained within some sort of packaging, e.g. pipes or panels. The containers needs to be designed so that they do not affect the original properties of the building material. Due to the large difference in total surface area of the PCM between micro and macro scale, the heat transfer is significantly better for micro scale integration compared to the macro scale (18).



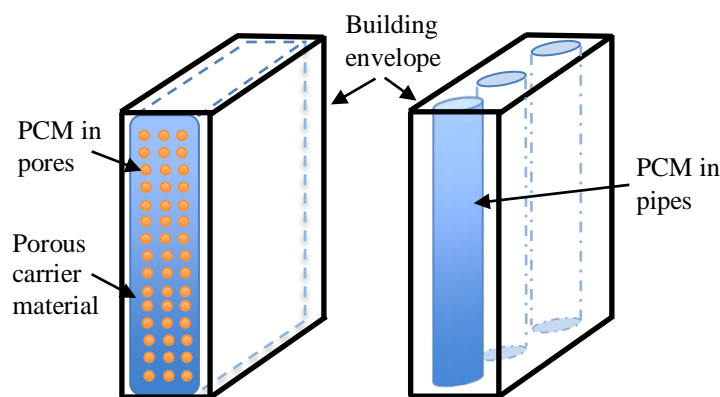***Figure 5:*** *This figure shows two different integration arrangements of PCMs in buildings. To the left, the PCM is integrated in the pores of a porous carrier material (micro scale). To the right, the PCM is contained in pipes (macro scale).*

# 3. Applied Methods for State of Charge Measurements

To determine the SOC of PCMs, the energy content has to be measured during phase transitions. In contrast to sensible heat storage materials where the material is either completely in liquid or solid form, PCMs also have a large LH storage that cannot be measured accurately using merely temperature sensors, due to the isothermal conditions (further described in section 2.1). To be able to measure transition enthalpies correctly it is important to be able to distinguish the amounts of the material that is either in its liquid or solid state (7). In the following section, a number of currently applied techniques for SOC measurements will be described. However, not all of these techniques will be experimentally evaluated in this study.

## 3.1. Thermal Methods for State of Charge Measurements

### 3.1.1. Differential Scanning Calorimetry

A common method for thermal analysis of PCMs is differential scanning calorimetry (DSC). This method measures the amount of heat absorbed or released by a sample during temperature change. A small sample (a few micrograms) is placed inside a hermetically sealed pan and put into a furnace chamber within the DSC apparatus. Next to the pan containing the sample, an identical empty pan is placed in a similar position, and used as a reference. The temperature development and specific thermal resistance ($r$) of the sample is measured by temperature sensors (during heating or cooling) and compared to that of the reference. This makes it possible to accurately measure the heat flow. The deviation between the temperature of the sample and the reference is measured and used to determine the heat flux between the sample and the furnace, allowing calculation of the sample enthalpy (19; 20).

The heat flux ($\dot{Q}$) is determined by knowing the specific thermal resistance of the reference ($r$) and by measuring the temperature difference between the sample and the reference, according to:

$$\dot{Q} = \frac{\Delta T}{r} \qquad\qquad (iii)$$

Where $\Delta T$ is the temperature difference between the sample and the reference.

$$\Delta T = T_{sample} - T_{reference} \qquad\qquad (iv)$$

A typical result from a DSC measurement where a PCM has been exposed to both heating and cooling can be seen in figure *6*. The peaks B and D shows the crystallization and melting temperatures, respectively, and the area under the peaks corresponds to the crystallization and melting enthalpies. The "exo-arrow" seen in figure *6* shows the exothermal energy direction, i.e. in what direction energy is released. The opposite direction corresponds to the endothermal direction i.e. in what direction energy is absorbed (13).
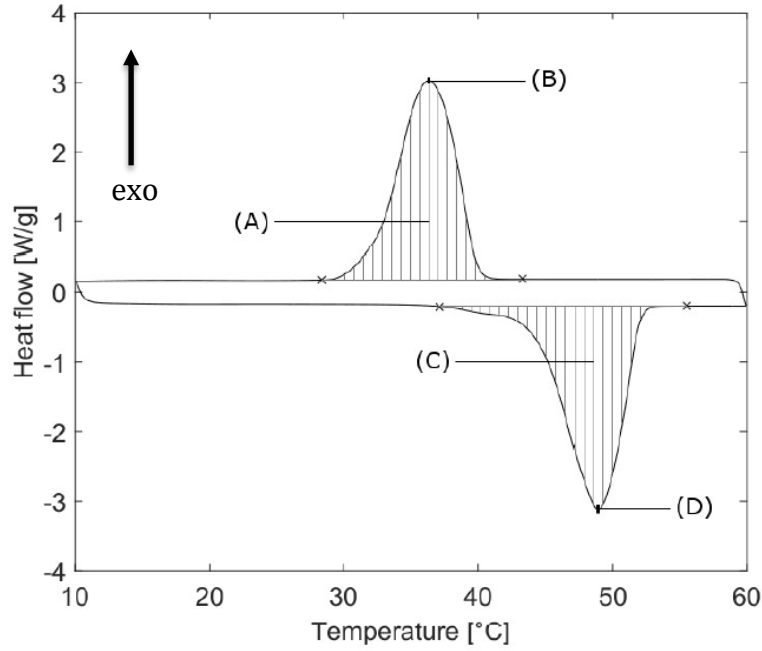
***Figure* 6**: *This figure shows five areas of interest when evaluating DSC data.* ***A***: *The lined area is the enthalpy of crystallization,* $\Delta H_c$. ***B***: *The highest point of the curve is the crystallization temperature,* $T_c$. ***C***: *The lined area is the enthalpy of melting,* $\Delta H_m$. ***D***: *The lowest point of the curve is the melting temperature,* $T_m$. *The temperature difference between B and D, is the subcooling.*

### 3.1.2. Dynamic Heat Flow Meter Apparatus

As mentioned above DSC is only valid for small samples, which makes it unsuitable for large scale building applications. A new technology, dynamic heat flow meter apparatus (DHFMA), has been developed that can be used to appropriately determine the SOC of PCMs in building envelopes. The DHFMA utilize information, such as temperature and other thermal information, from the heat flow meter apparatus (HFMA) to determine the dynamic properties of the PCM (6). The HFMA is used to measure steady-state thermal properties at different temperatures. A HFMA consists of two plates with heat flux transducers on each plate and the temperature is controlled using thermoelectric elements and water coolers. In a HFMA the plates have different temperatures to create a temperature gradient, whereas in the DHFMA the temperatures are set to the same value. Thermal equilibrium are obtained at each temperature step. The temperature and heat flow rates are logged at each time interval via the heat flow transducers and thermocouples for the two plates, top and bottom ($Q_{top}$ and $Q_{bot}$). The enthalpy ($H$), in terms of heat per unit square of surface area, is determined by integrating heat flow rates over time ($\tau$) expressed as (21):

$$H = \Sigma\left[H_i + \left[(Q_{top,i} - Q_{top,f})s_{top} + (Q_{bot,i} - Q_{bot,f})s_{bot}\right]\tau\right] \qquad (iv)$$

Where $s$ is the calibration factor and the indexes $i$ and $f$ indicates initial and final conditions respectively. The effective volumetric heat capacity ($C_{eff}$) of a PCM enhanced building envelope can be defined as the derivative of the enthalpy with respect to the temperature and gives:

$$C_{eff} = \frac{1}{L}\frac{dH}{dT} \approx \frac{1}{L}\frac{H_{i+1}-H_i}{T_{i+1}-T_i} \qquad\qquad (v)$$

Where L is the thickness of sample (21).

### 3.1.3. T-History Method

Temperature history (T-history) is a method that is used for creating phase diagrams and records the temperature changes of a material as it is being cooled down. Changes of thermophysical properties (such as phase transitions) leads to a release of heat which results in a change of the temperature history. By measuring the temperature of a PCM and comparing it to a reference with known heat capacity (C), it is possible to calculate the generated heat flux. The heat transfer between the surroundings and the sample is assumed to be identical to the heat transfer between the surroundings and the reference (22). The heat flux from the sample is calculated according to:

$$\dot{Q} = \frac{1}{r}\left(T_{sample} - T_{ambient}\right) = -c_{sample}\frac{d}{dt}T_{sample} \qquad\qquad (vi)$$

If the sample and the reference have the same geometry and are placed in the same environment, the specific thermal resistance ($r$) is the same. Since the heat capacity of the reference is known, the specific thermal resistance can be determined from the following expression:

$$\dot{Q} = \frac{1}{r}\left(T_{reference} - T_{ambient}\right) = -c_{reference}\frac{d}{dt}T_{reference} \qquad\qquad (vii)$$

This method has been around since 1999 and is applicable for large (grams) inhomogeneous samples (22).

### 3.1.4. Transient Plane Source Technique

Transient plane source (TPS) technology measures the increase in sample temperature as a sample is exposed to a specified heat effect over a certain time period. The increase in sample temperature can then be related to various properties of the sample such as thermal conductivity, thermal diffusivity and volumetric heat capacity. TPS has been used in a previous study trying to correlate the differences in thermal properties to the SOC during phase transitions of salt hydrates (23). In that study a kapton (polyimide film) sensor was placed in between two layers of PCM and pressed tightly together by clamps. A constant electric power was then supplied through a thin (10 $\mu m$) spiral inside the sensor and the increase in sample temperature could be registered. The results of that study shows that it is possible to distinguish between the liquid and solid state of PCMs using the TPS technique, but that it has some limitations. The sensor is very sensitive to changes in temperature of the surroundings, consequentially there is a need for a completely temperature controlled environment in order for it to operate optimally. In addition it is important to ensure good contact between the sensor and the PCM to obtain reliable results (23).

## 3.2.    Physical Methods for State of Charge Measurements

### 3.2.1.    Measurements of Volumetric Change

Previous studies have been made utilizing the fact that physical and chemical properties changes during phase transitions. As a PCM undergoes a phase transition, either from solid to liquid or from liquid to solid, a change in the volume of the material occurs. The volume of the PCM increases as it goes towards liquid state. If the PCM is encapsulated within a closed system this will also result in an increased air pressure inside the PCM container, see figure 7. However, the air inside the closed storage system will also change in volume as the temperature changes. By measuring both the internal temperature and pressure it is possible to calculate a relationship between these properties, which later can be correlated to the SOC. This method is relevant for PCMs showing large differences in volume between their liquid and solid state, such as paraffins (7).
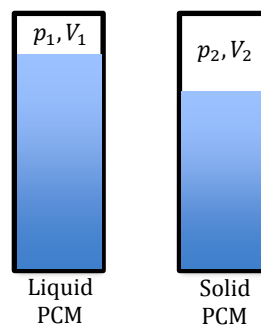


*Figure 7: This figure shows how the volume changes for a PCM in liquid and solid state. By measuring the pressure and the temperature inside the container it is possible to calculate the volume change and later correlate it to the SOC.*

### 3.2.2.    Measurements of Dampening Effects

Another method is to let mechanically induced acoustic waves propagate through the PCM during phase transitions and measure the change in propagation speed and dampening of the signal. These changes varies strongly depending on if the material is either in liquid or solid state and is therefore related to the SOC. One advantage with this method compared to thermal methods is that it requires only one type of sensor (measuring the signal) instead of multiple local sensors measuring the temperature and the heat flow, thus making it a cost effective alternative. Furthermore, this method is applicable for all types of PCMs (7).

### 3.2.3.    Measurements of Viscosity Changes

The viscosity of a material will change during a phase transition and it can be measured by two different methods, viscometers or rheometers. The viscometers are generally used for fluids whose viscosity is constant during varying flow conditions (i.e. laminar or turbulent flow), while rheometers are used when the fluid has changing viscosity as the flow conditions varies. There are several types of viscometers available for laboratories, e.g. falling spheres and piston viscometers, rotational viscometers, bubble viscometers and orifice viscometers. The latter is easy to operate and measures the viscosity as a time of flow. An example of an orifice viscometer is a Redwood viscometer which was developed in 1937 and measures the time it takes to empty a specific volume of the fluid from a container

(24). However when the viscosity changes as a consequence of temperature change, a rheometer is more suitable as it can easily be equipped with a heating- and cooling system (25).

### 3.3. Dielectric Spectroscopy

Dielectric spectroscopy (also called impedance spectroscopy) measures the dielectric properties of a material as a function of electric frequency. The interactions between an external electric field, generated over two electrodes, and the electric dipole moment of the different sample molecules are measured. These interactions relates to the impedance spectrum of the sample (26). The dielectric spectroscopy measurement can be used to measure the materials structural properties like phase transitions, phase compositions and crystallization processes. It can also monitor chemical reactions, polymerization and be used for characterization of drugs etc. (27). The electric properties of the material, such as the conductivity ($\sigma$), can be calculated by knowing the strength of the generated electric field over the electrodes as well as the current density, according to:

$$\sigma = \frac{J}{E} \qquad\qquad (viii)$$

Where $E$ is the electric field and $J$ is the current density. Besides frequency, temperature is another important parameter when evaluating the electrical properties of a material during phase transitions (26). Since electrical properties are temperature dependent they vary naturally depending on the temperature of the material. This means that changes of electrical properties during heating or cooling does not necessarily indicate that a phase transition is occurring.

**CHALMERS** *Civil and Environmental Engineering*, Master's Thesis BOMX02-16-85

# 4. Methodology and Experimental

The experimental procedure throughout this Master's Thesis is illustrated in figure 8. The idea was to select a few PCMs from each of the investigated PCM types and create DSC references for each of these materials. Based on literature research, suitable methods for visualization of property changes, during phase transitions, were selected and tested experimentally for these materials. The results from each of these experiments were then compared to the corresponding DSC reference for that specific PCM. Based on the conformity to the DSC reference, conclusions could be drawn whether the selected method was reliable or not.
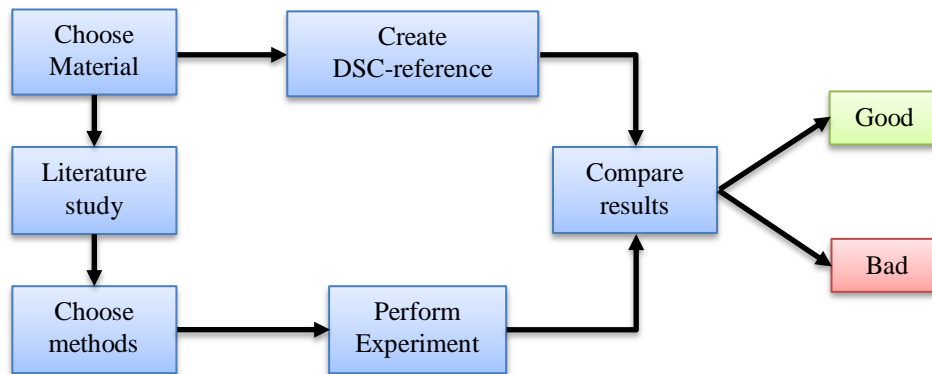


**Figure 8:** *This figure shows the experimental methodology used during this Master's Thesis.*

Most of the equipment needed to carry out the experiments conducted in this study was available at Chalmers University of Technology such as the rheometer, density meter, DSC and dielectric equipment. However some techniques, such as the light transmittance device and the electrical resistance equipment (which can be related to the dielectric method) had to be designed on site in order to serve as good performance indicators. All of these techniques will be further described in this section along with a description of the materials used for the experiments.

## 4.1. PCM Chemicals

Two types of organic PCMs were analyzed in this study, polyethylene glycol (PEG, of different grades) and sugar alcohols. The PEGs had a molecular weight of either; 600, 1000, 1500, 4000 or 6000 $g/mol$. The sugar alcohols were xylitol and erythritol, which both have relatively low melting temperatures considering that they are sugar alcohols (which normally have melting temperatures around 150 °C). The large temperature difference between melting and crystallization of erythritol is due to substantial subcooling when performing DSC analysis, which also have been observed in a study made by Hayashi et al. (28). All chemicals were laboratory graded and provided by Fisher Scientific®. The inorganic PCMs, investigated in this study, were provided by the company Climator Sweden AB® who specializes in producing energy storing materials. Their product is called ClimSel™ and is a salt hydrate that can be modified to have transition temperatures in the interval -21° to 70°C. The ClimSel™-PCMs investigated in this study had transition temperatures of either 28°C or 58°C and are called C28 or C58 respectively. The exact

composition of the commercial product ClimSel™-PCMs is unknown. The transition points and the heat of fusion for the PCMs can be found in Table 1.

**Table 1:** *This table shows the melting temperature, crystallization temperature or transition temperature as well as the heat of fusion for the investigated PCMs.*

| Compound | Melting Temperature [°C] | Crystallization Temperature [°C] | Heat of Fusion [kJ/kg] |
|---|---|---|---|
| **Organics** | | | |
| PEG600 | 19.7 | 10.6 | 119.5 |
| PEG1000 | 37.1 | 33.4 | 151.9 |
| PEG1500 | 47.6 | 39.6 | 161.3 |
| PEG4000 | 60.9 | 44.5 | 170.3 |
| PEG6000 | 61.1 | 46.2 | 180.1 |
| Xylitol | 94.2 | -* | -* |
| Erythritol | 119.6 | 27.6 | 281.8 |
| **Inorganics** | | | |
| C28 | 31.6 | 24.1 | 86.0 |
| C58 | 59.2 | 52.4 | 232.2 |

\* No crystallization occurred when running DSC-measurements, thus unable to determine crystallization temperature and heat of fusion

## 4.2.  Analytic Equipment

### 4.2.1.  Calorimetric Analysis

Thermal evaluation of the investigated PCMs was conducted using a differential scanning calorimeter (DSC 1, Mettler Toledo®, see section 3.1.1. for function description) equipped with a cooling compressor. Small samples in the range of 10-30 mg were heated above their melting point and then cooled again below their crystallization point, this will be referred to as a thermal cycle and is illustrated in figure *6*. To approximately simulate the temperature change of ambient cooling in room temperature, the temperature change within the DSC was set to 1 °C/min (This was done in order to correlate other experimental results to DSC data). An average obtained from 3 thermal cycles was calculated to serve as a base for how the thermal behavior of the PCMs changes during the transitional states. Many PCMs shows a deviation between the first thermal cycle and the subsequent cycles. This phenomena is likely to be caused by changes in thermal resistance between the cycles. The change in thermal resistance is due to a change in contact area between the sample and the bottom of the pan as the sample melts and crystallizes. For instance, if the sample is put into the pan as a solid, there will be some empty space in between the bottom of the pan and the sample since it will be porously packed. As the sample melts, it floats out and covers the entire bottom area of the pan resulting in a change in contact area and therefore a change in thermal resistance. This results in a slight dislocation of the melting temperature compared to the initial thermal cycle (29). Since this effect is only noticeable during the first cycle, those results were removed when calculating the average results. The final results (which are averages of 3 cycles) were used as a reference to other analytic measurement techniques to verify their accuracy and reliability.

### 4.2.2. Density Analysis

Density measurements were performed using an Anton-Paar density meter (DMA 4500M®), seen in figure 9. A small liquid sample of approximately 1ml was injected into a so called oscillating U-tube sensor. The instrument electronically excites the U-tube sensor to simultaneously oscillate at the fundamental resonant frequency and its harmonics. The oscillation characteristics are measured with an integrated reference oscillator providing the pace. The reference oscillator is positioned in close thermal contact with the oscillating U-tube. This positioning enables the reference oscillator to compensate for all drifts arising from temperature stress. The density is determined with great accuracy, including correction of the viscosity influence (30). Measurements were taken in steps of 0.5 °C during a temperature ramp, starting at a temperature where the PCM was completely in liquid state and the cooled until it was completely solid.
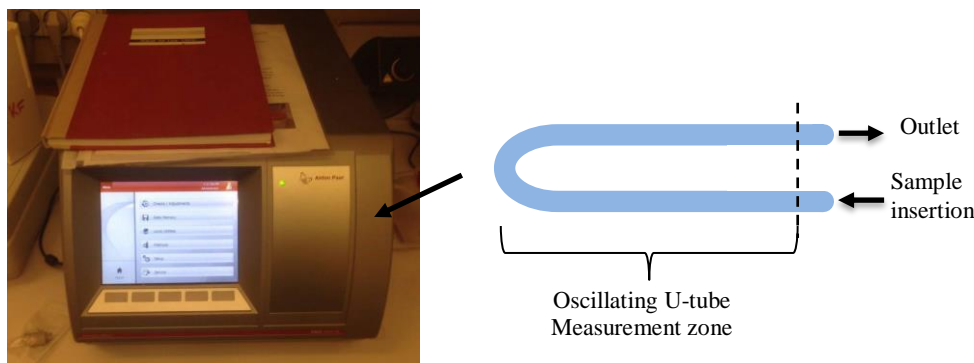


*Figure 9: This figure shows a photo of the Anton-Paar density meter (left), used for the density measurements. A sketch of the oscillating U-tube sensor, into which the sample was injected, can be seen to the right. The U-tube sensor is located on the side of the density meter and is integrated into the apparatus.*

### 4.2.3. Viscosity Analysis

The viscosity measurements were performed using a rheometer from Bohlin Instruments (CVO 200®) equipped with a cooling/heating system. About 100 ml of melted PCM sample was added into the sample cup of the equipment. The rotor was equipped with a bob that was submerged into the sample, see figure 10. The rotation speed was set to a constant shear rate during the test cycle. A temperature ramp was applied, with the same cooling and heating rate as used for the DSC measurements (1 °C/min). Initially the sample was cooled down below its crystallization temperature and then heated up again to above its melting temperature while continuously measuring the shear stress during the test cycle.
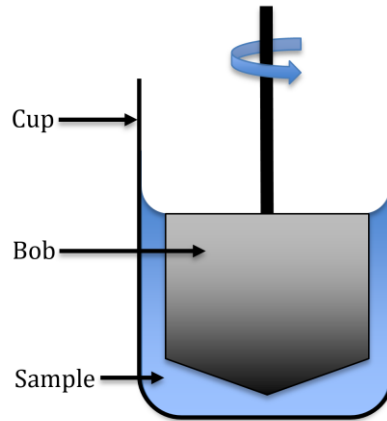
*Figure 10: This figure shows a schematic setup for the cup and bob for viscosity measurement. Recreated from Rheosys LLC (25).*

### 4.2.4. Optical Analysis

The optical setup, which is illustrated in figure 11, made it possible to measure the amount of light that was transmitted through a material during crystallization. Light was focused by a lens to hit the center of a cuvette filled with a PCM sample of 3.5 ml. Behind the cuvette, a light sensor (HAGNER® EC1) was placed to measure the amount of light that was able to penetrate the sample. The experiments were performed in a dark room at 21°C and the light source used was a white light lamp (1.5-W LED, 230-240V and 50Hz).
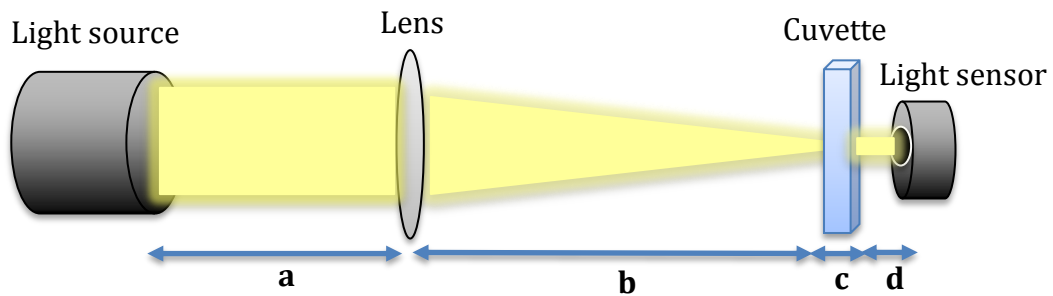


*Figure 11: This figure shows the setup for the illuminance measurement of the PCMs. The length of **a** = 40 cm, **b** = 94 cm, **c** = 1 cm and **d** = 0.5 cm.*

Each PCM sample was initially heated above its melting temperature using a hot plate. The melted sample was then removed from the hot plate and poured into a cuvette. The cuvette was then cooled down by the ambient air below its crystallization temperature. During this time, measurements were performed measuring the temperature and the illuminance at every 20 second. However, for erythritol, measurements had to be performed while the cuvette was still on the hot plate since crystallization occurred as soon as it was poured into the cuvette. The sample temperature was estimated by measuring the surface temperature of the cuvette using an infrared (IR) camera. A photo of the setup is seen in figure 12.
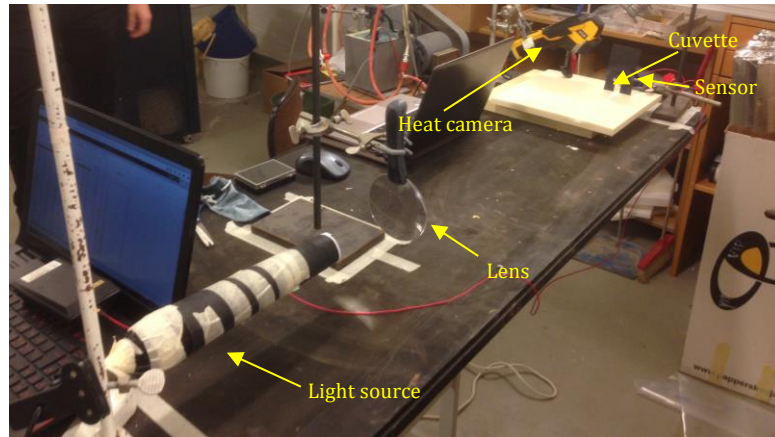
***Figure 12:*** *This figure shows a photo of the experimental setup for the illuminance measurements. All components were fixed by supports and clamps to ensure uniform positions for all measurements.*

### 4.2.5. Electrical Resistance Analysis

An electrical setup was built to enable measurements of how the electrical resistance of a PCM changes during crystallization. The idea was to melt a PCM sample on a hotplate and then let a known current from a set voltage source (0.5A alternating current and 10V) pass through the melted sample during cooling and crystallization. By connecting a multimeter to the circuit, the current that was able to pass through the sample could be measured and logged regularly. The current passing through the sample ($I$) is directly related to the electrical resistance ($R$) of the material by Ohms law:

$$R = \frac{U}{I} \qquad\qquad (ix)$$

Where $U$ is the voltage over the circuit.

A sketch of the wiring diagram and a picture of the actual setup is seen in figure 13. Samples of sizes between 40-50 ml were melted in a glass beaker and then cooled by the ambient air (of approximately 20 °C) until crystallization occurred. The electrodes used for this experiment were made out of zinc coated copper and were fixed to the inner walls of the glass beaker using electrical tape. An IR-camera was used to determine the temperature of the sample. The current passing through the sample was measured at every 20 second along with the temperature throughout the experiment.
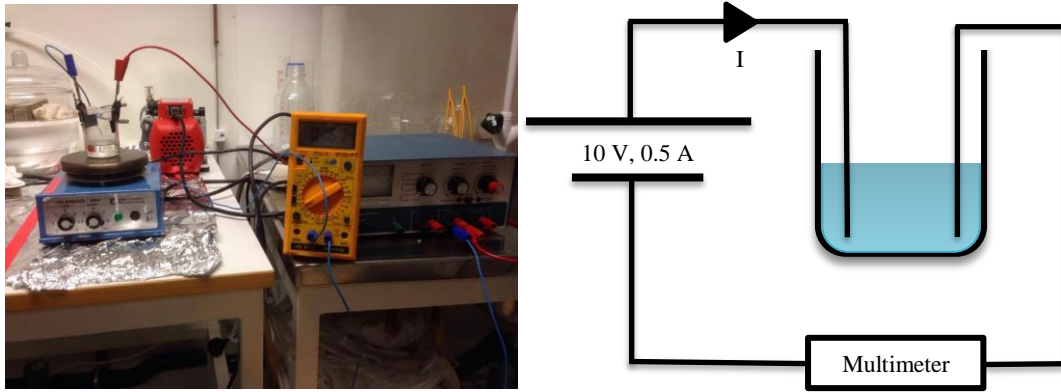
*Figure 13: The figure shows a photo of the setup as well as the wiring diagram for the resistance measurements. The multimeter was set to measure the current.*

### 4.2.6. Dielectric Spectroscopy Analysis

The dielectric spectroscopy were performed using a broadband dielectric spectrometer from Novocontrol GmbH, seen in figure 14. The sample cell was prepared by adding material into the cell, according to figure 15. Before closing the cell the material was melted to ensure good contact between the electrodes and the material. Additionally, some silicon spacers (diameter of $100 \ \mu m$) were added between the two electrodes to prevent the electrodes to get in contact with each other as the material melts throughout the test. Then by placing the second electrode on top, the cell was closed. The tested frequencies were set to 40, 50 and 60 $Hz$ to be in the same range as the frequency found in regular household sockets. The temperature varied between 0-150 ℃ to be able to measure the conductivity both during melting and crystallization for the different PCMs, starting with the melting and then the crystallization.
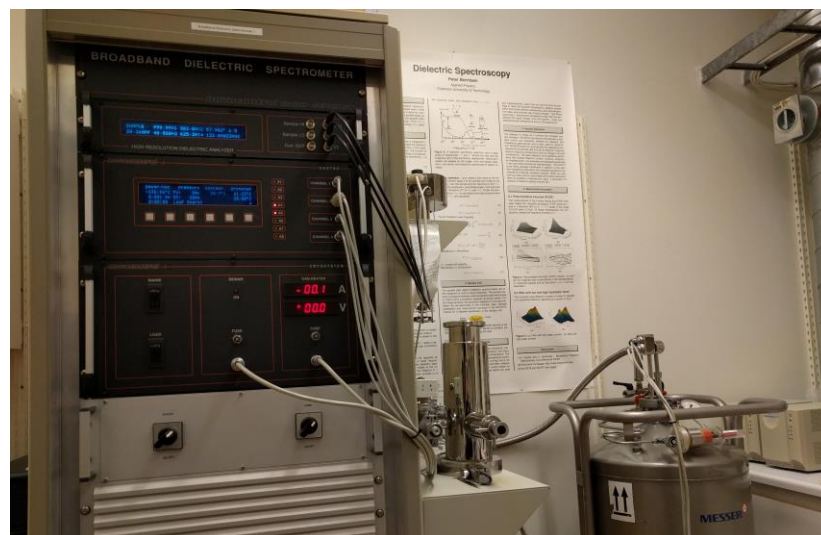


*Figure 14: This figure shows a photo of the broadband dielectric spectroscopy equipment from Novocontrol, equipped with a nitrogen gas heating/cooling system.*
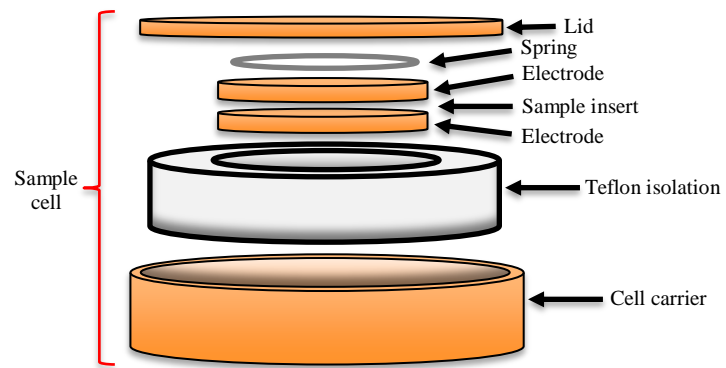
**Figure 15:** *This figure shows a sample cell used for the dielectric spectroscopy measurement for materials that can be either in liquid or solid state. The lid, electrodes and the cell carrier were made of brass. The spring is used to ensure connection between the top electrode and the lid*

# 5. Results and Discussion

## 5.1. Calorimetric Measurements

The results from the DSC measurements were obtained following the procedure described in section 4.2.1. These results are used as a reference to compare results obtained by other methods to validate their reliability and accuracy throughout this section. Complete DSC figures can be found in appendix A for all investigated PCMs apart from xylitol, for which no complete DSC data could be obtained. This is due to its formation of a highly viscous metastable state during cooling instead of crystallizing (resulting in a non-observable crystallization peak when performing DSC analysis).

## 5.2. Viscosity Measurements

PEG600 (which has a melting temperature of 20.7 °C) was poured into the cup of the rheometer and cooled down to 5°C and then reheated up to 25°C. The viscosity was measured continuously during the experiment and then compared to corresponding DSC data, seen in figure 16.
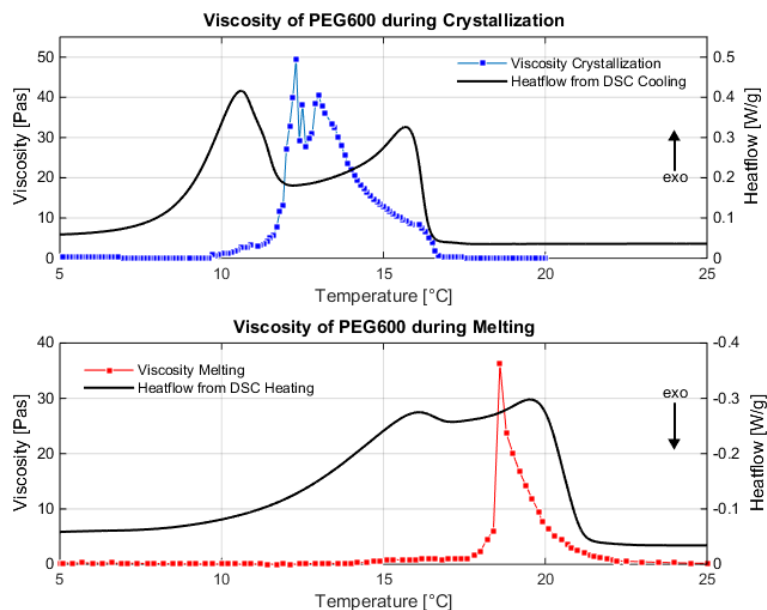


***Figure 16:*** *This figure shows the how the viscosity of PEG600 changes during melting and crystallization. The viscosity reaches a peak of 50 Pas at 12 °C during the crystallization which is right in between the two DSC peak (top panel). The viscosity peak at 18 °C during the melting corresponds reasonably well with the DSC curve that shows a melting temperature between 15-20 °C (bottom panel).*

The increase in viscosity of PEG600 during crystallization was expected, however the drop in viscosity that followed the peak was not. In theory, the viscosity should approach infinity when a material solidifies. Therefore, for this experiment, the viscosity was assumed to reach a maximum value as the sample approaches complete crystallization and then to remain around that value upon further cooling. As a consequence, the viscosity peak seen in the melting region was also unexpected. Another measurement was performed on PEG1000 to see if this effect

was reoccurring. The results can be seen in figure 17, where the same behavior was observed. The viscosity of PEG1000 reaches a peak in the region of crystallization and then drops down significantly and remains at low levels (around 3 Pas) during further cooling. Upon heating, the viscosity forms three distinct peaks between 30-36 °C before leveling out again at low viscosity values.
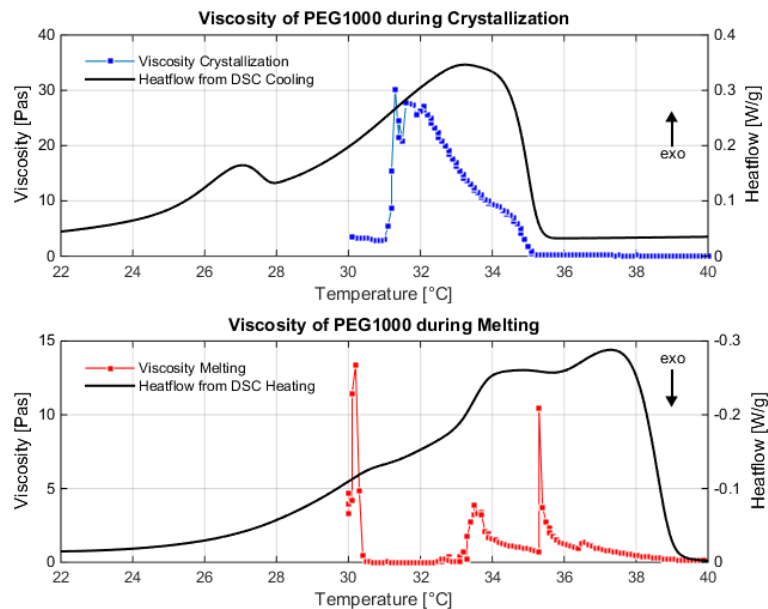


*Figure 17: This figure shows how the viscosity of PEG1000 changes during melting and crystallization. The viscosity reaches a peak of 30 Pas at 31.4 °C during crystallization and then drops down to 3 Pas (top panel). Upon heating the viscosity shows three peaks at 30 °C, 33 °C and 35°C all within the region of melting shown by the DSC curve (bottom panel).*

When studying the sample inside the rheometer closely during the measurements an air-gap could be seen between the rotating bob and the inner walls of the cup. As the bob rotates it pushes the waxy sample upwards over the bob and upon the walls of the cup, thus forming an air-gap, seen in figure 18.
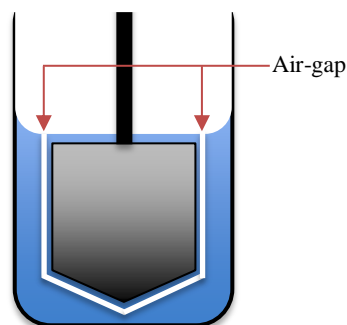


*Figure 18: This figure show an illustration of the air-gap formed during the crystallization when performing the viscosity measurements.*

This explains the sudden drop in viscosity that occurs after crystallization as well as the formation of different peaks during melting. As the air gap starts to form during crystallization, the rotating bob loses contact with the sample inside the cup, resulting in viscosity measurements on the surrounding air instead. This makes the viscosity drop. As the sample is being reheated and begins to melt, the contact

between the bob and the sample is reestablished resulting in a viscosity peak. Before the sample reaches a completely liquid state, the bob may continue to push the sample upwards, creating another air-gap which can give rise to additional viscosity peaks. Once the sample is completely melted, no additional air-gaps could form since there is continuous contact between the sample and the rotating bob. Figure 19 shows how the viscosity of the salt hydrate C28 changes during crystallization.
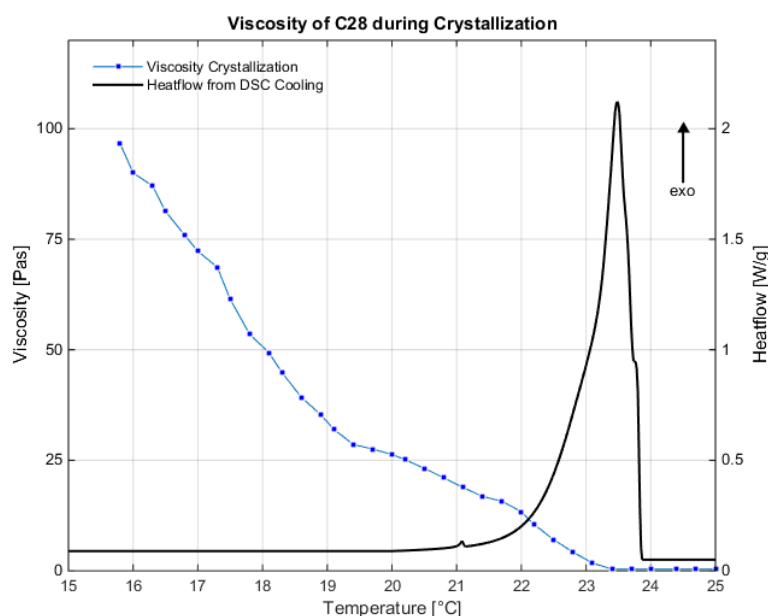


**Figure 19:** *This figure shows how the viscosity of C28 changes during crystallization. The viscosity of C28 gradually increases upon cooling after reaching the crystallization temperature indicated by the DSC curve at 24.1 °C. The crystallization region is seen to be significantly longer during the viscosity measurement compared to the DSC curve.*

In contrast to the results of the PEGs, no drop in viscosity was observed for C28 upon crystallization. Salt hydrates form much harder "rock like" crystals compared to the waxy solids formed by the polymers. These hard crystals prevents the bob from rearranging the material and thus preventing the formation of air-gaps to the same extent as observed for the PEGs. The crystals eventually creates enough resistance to completely stop the rotation of the bob, forcing a shutdown of the measurement. This can be seen in figure 19 at about 16 °C, reaching a maximum viscosity of 98 *Pas*. The reason for why the viscosity continues to increase well below the crystallization temperature indicated by the DSC is unclear. Both during the viscosity measurement and during the DSC analysis the cooling rate was pre-set to 1 °C/min and thus they should indicate the same crystallization temperature. One possible explanation is that the chemical composition of the C28 may have changed due to evaporation of volatile compounds during the melting of the sample prior to the experiment. This may have affected the crystallization temperature of the C28. Throughout the experiment the cup was covered with tape trying to minimize the exposure to the surrounding air, only leaving a small gap in the tape for the rotor to be able to rotate. This seal was surely not completely air-tight which may have affected the chemical composition of the C28. Another reason could be the difference in sample size between the experiments (grams in the rheometer

compared to micrograms in the DSC), which has been observed to have a significant influence on the crystallization temperature for certain PCM types (i.e. the sugar alcohol erythritol) (28).

The temperature region in which the rheometer can operate is approximately 0-70 °C due to limitations of the heat transfer medium inside the equipment. This restriction made viscosity measurements of sugar alcohols impossible due to their high melting temperatures. Attempts were made trying to melt erythritol on a hotplate prior to the measurements and solely measure the viscosity upon crystallization. However, the crystallization of the erythritol was initiated almost immediately after being poured into the cup, before viscosity measurements could begin.

### 5.3. Density Measurements

Density measurements were conducted using an Anton-Paar density meter (further described in section 4.2.2). Figure 20 shows the results from the measurement performed on PEG600 during crystallization as it was cooled down from 30 °C to 5 °C. The density of PEG600 increases linearly during cooling until reaching approximately 18 °C. At this point a more rapid increase in density is observed, reaching a maximum of 1.138 $g/cm^3$ close to 16 °C. Then the density drops down upon further cooling.
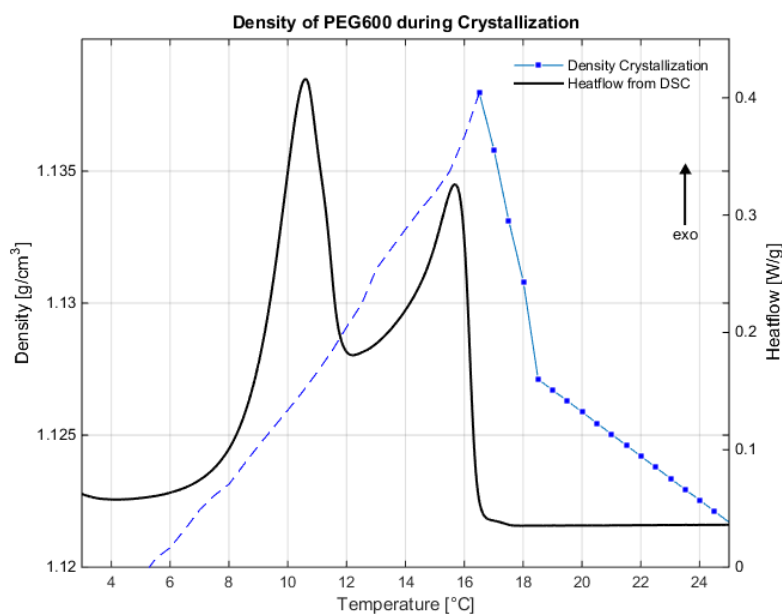


***Figure 20:*** *This figure shows the change in density of PEG600 during crystallization. The density increases linearly during cooling between 25-18 °C, then a more rapid increase is seen followed by a peak of 1.138 $g/cm^3$ at 16 °C. The density then drops down again upon further cooling. The peak in density corresponds reasonably well to the peak at 15.8 °C shown by the DSC curve.*

The density of the polymer was expected to increase during crystallization, however the sudden drop in density after the peak (the dashed line in figure 20) was not expected. As the polymer reaches complete crystallization, the density was assumed to level out and remain at a maximum density level that corresponds to that of the solid material. The Anton-Paar density meter is normally only used to measure the density of liquids and gasses and not solid materials (since the data is not reliable

according to the manufacturer). This is most likely the cause of the unexpected behavior observed after the peak during crystallization (30). A similar behavior is seen for PEG1000 in figure 21. The density increases linearly during cooling until reaching the crystallization temperature at approximately 34 °C. The density then drops down upon further cooling.
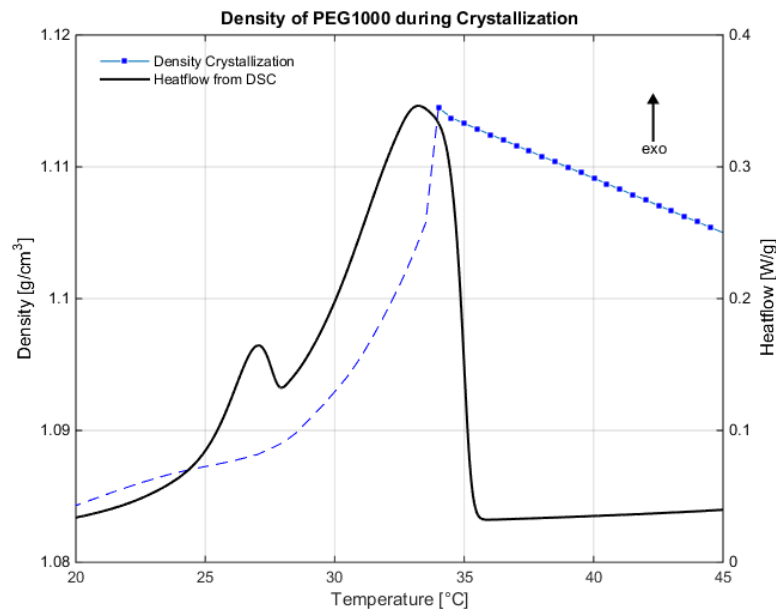


*Figure 21: This figure shows the change in density of PEG1000 during crystallization. The density increases linearly during cooling between 45-34 °C, reaching a maximum value of 1.115 g/cm³ at 34 °C. The density then drops throughout the crystallization. The density peak matches the corresponding crystallization peak from the DSC at 33.4 °C reasonably well.*

For both PEG600 and PEG1000 the density peaks co-occurs with the heat flow peaks from the DSC at the crystallization temperature, seen in figure 20 and figure 21. This verifies that the maximum density is achieved at the crystallization temperature. The density drop upon further cooling below the crystallization temperature is most likely a result of inaccurate data obtained from the density meter (explained above).

The sample had to be injected by a syringe into the density meter, therefore it had to be melted prior to insertion. The machine can only operate in a temperature range of approximately –20 °C to 90 °C and it is sensitive to corrosive materials. Those restrictions excluded measurements on sugar alcohols due to their high melting temperature, and on salt hydrates due to their corrosiveness.

## 5.4. Light Transmittance Measurements

A significant drop in light transmittance was observed during crystallization for all PEGs tested (PEG1000, PEG1500, PEG4000 and PEG6000). The light transmittance then levels out as the PEGs approaches complete crystallization. The results from the measurements were compared with corresponding DSC curves for the materials, with approximately the same cooling rate. Time marks were used to visualize the crystallization times for both the light transmittance measurement and the DSC curves. Figure 22 shows the change in light transmittance through PEG1000 during crystallization (an enlarged graph can be found in appendix B).
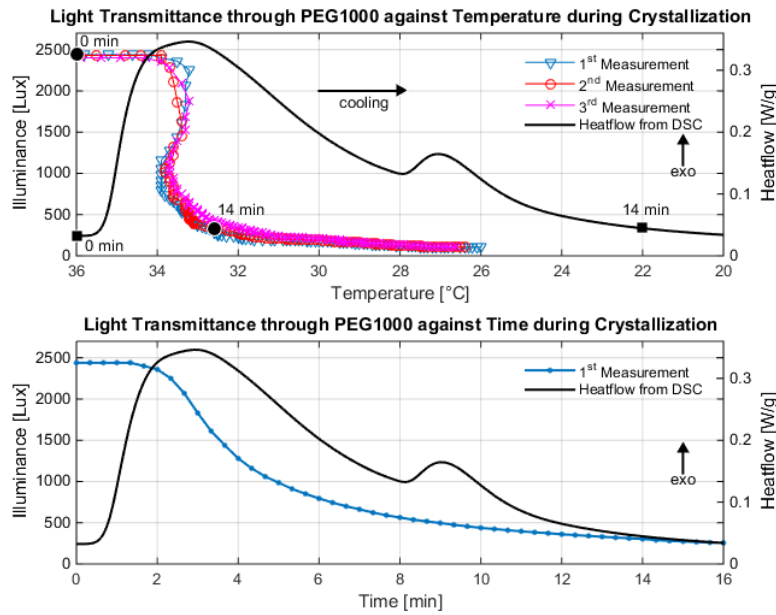
***Figure 22:*** *This figure shows the results from three light transmittance measurements of PEG1000. The upper panel shows the light transmittance plotted against the temperature. The bottom panel shows the change in light transmittance from the first measurement plotted against the time.*

For PEG1000, the light transmittance remains constant at approximately 2450 lux as the polymer is in its liquid state, i.e. above 34 °C. As the crystallization starts, the light transmittance drops continuously, close to the crystallization temperature. After 14 minutes approximately 95% of the polymer is in its crystalline state. These results suggests that the light transmittance is directly related to the degree of crystallinity of PEG1000. The reason for the difference in temperature between the DSC curve and the light transmittance measurements 14 minutes into the experiment (seen in the upper panel of figure 22) is due to the LH released during crystallization affecting the temperature of the sample. In the DSC, this release of heat does not affect the temperature of the sample since the apparatus is set to maintain a cooling rate of 1 °C/min (the DSC just provides additional cooling to maintain these settings). However, during the light transmittance measurements the LH heats up the sample (since the sample is only exposed to ambient cooling), making the temperature remain higher throughout the crystallization. This effect is even more visible for PEG1500 as seen in figure 23.
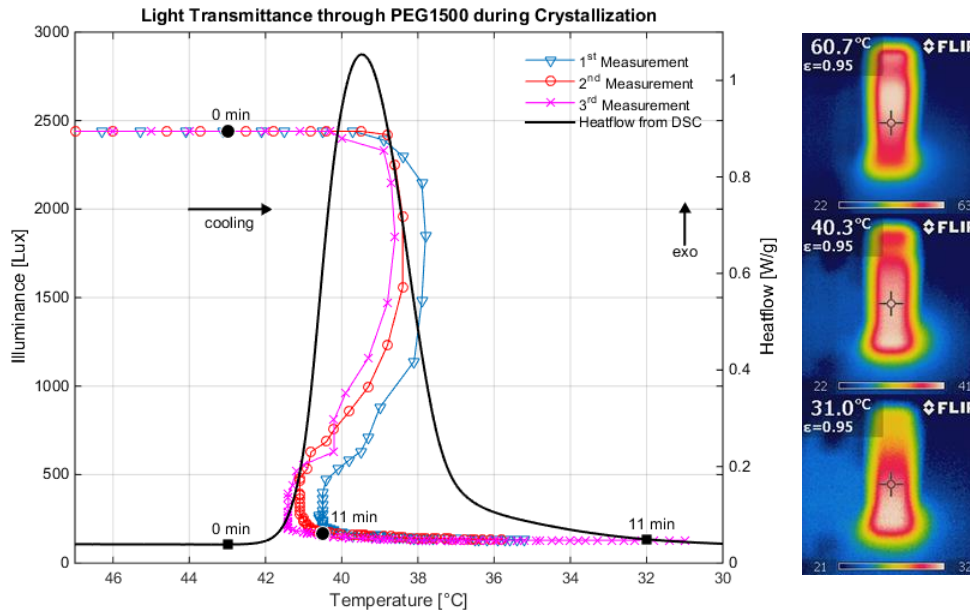
***Figure 23:*** *This figure shows the results from three light transmittance measurements of PEG1500 plotted against the temperature. Pictures of the sample, taken by the IR camera are seen to the right, one fully liquid (60.7 °C), one partly crystallized (40.3 °C) and one completely crystallized (31.0 °C) after approximately 11 minutes.*

As observed also for PEG1000 (in figure 22), the light transmittance remains constant at approximately 2450 lux as PEG1500 is in its liquid state, i.e. above 40 °C. As the crystallization starts, the light transmittance drops continuously and the LH released during crystallization results in an increase of the sample temperature. Both of these effects (the drop in light transmittance and the increase in sample temperature during crystallization) were also observed for PEG4000 and PEG6000. The results from the light transmittance measurements of these two polymers can be found in appendix C along with complementary time plots for PEG1500, PEG4000 and PEG6000.

The polymers are completely transparent in their liquid state, thus allowing most of the incoming light to pass through the sample (approximately 2450 lux). As the crystallization starts, crystal seeds starts appearing throughout the sample, growing rapidly until eventually the entire sample becomes an opaque, waxy solid. The light transmittance in this state is much lower compared to its liquid state, letting only a small portion of the light to pass through the sample (approximately 100 lux).

Light transmittance measurements were also performed on the sugar alcohols xylitol and erythritol. Erythritol shows a significant drop in light transmittance similar to the PEGs and can be seen in figure 24. A time plot for erythritol can be found in appendix C, which shows how the light transmittance changes during the crystallization time.
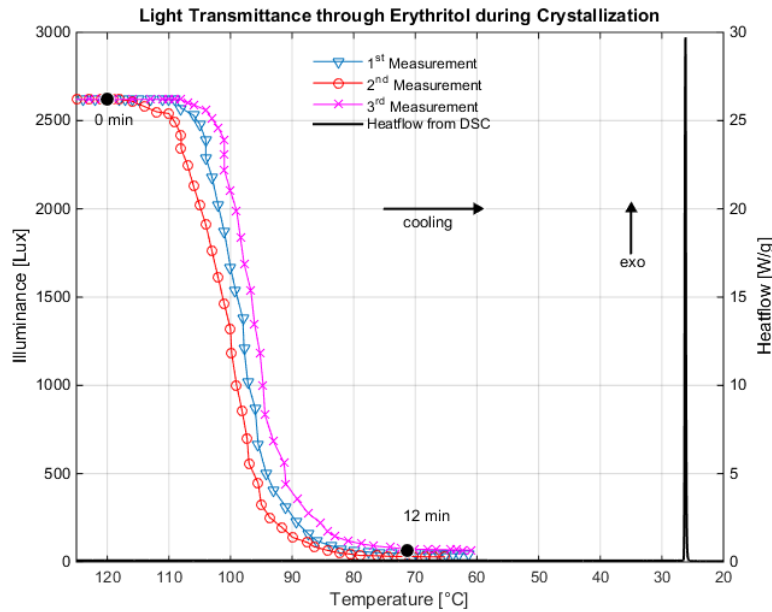
**Figure 24**: *This figure shows the results from three light transmittance measurements of erythritol plotted against temperature. The illuminance drop is seen to occur at a temperature between 100-110 °C which is significantly higher than the crystallization temperature indicated by the DSC curve at 27.6 °C.*

It is notable that the crystallization occurs at a much higher temperature than what is indicated by the DSC curve (around 100 °C instead of 27.6 °C). A possible explanation for this could be that the setup of the equipment for erythritol was slightly different due to the high melting temperature of the material. The cuvette was placed on a hot plate and the material was melted inside the cuvette. This difference in setup can influence the temperature measurements during the test due to the heat produced by the hot plate. However it is considered unlikely that the heat produced by the hotplate could affect the temperature measurements with the IR camera to such a large extent. There is also clear difference in sample volume between the optical measurements and the DSC (grams instead of micrograms), which is strongly related to the degree of subcooling for erythritol according to Hayashi et al. (28). This may explain the differences in crystallization temperature between the two measurements. However, the differences in sample volume is not seen to affect the crystallization temperatures of the PEGs.

As mentioned in section 2.3, xylitol adopts an amorphous metastable state during cooling, as shown by the lack of a crystallization peak in the DSC scans. Similarly, no crystallization of xylitol was observed during the light transmittance measurements. Instead it remained in its amorphous metastable state throughout the experiment. Since no crystals formed and the liquid was completely clear, no drop in light transmittance was observed and the light transmittance remained high at 2450 lux.

The salt hydrates are inhomogeneous and "grainy" in their liquid state which translates into relatively poor light transparency. To be able to perform optical measurements on the salt hydrates more light was focused onto the sample and some of the light shielding equipment was removed to further maximize the amount of ingoing light. This is the reason for why the light transmittance starts at a lower value (550 lux) for the C58 seen in figure 25.
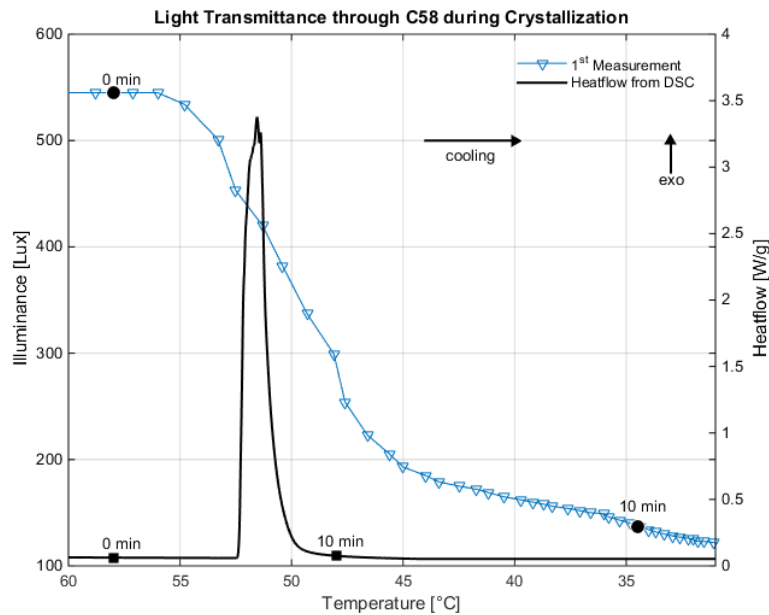
***Figure 25***: *This figure shows the results from the light transmittance measurement of C58 during crystallization plotted against the temperature. The drop in light transmittance starts at approximately 55 °C, which is a few degrees higher than the crystallization temperature indicated by the DSC (at 52.4 °C).*

The drop in light transmittance is seen to start at approximately 55 °C which is close to the initial crystallization indicated by the DSC curve at 52.4 °C. The drop lasts for about 10 minutes which also corresponds well to the crystallization time in the DSC. The reason that the salt hydrate C58 was chosen for this experiment is because of its high crystallization temperature (52.4 °C) in comparison to the C28 (24.1 °C). Since the samples were cooled down by the ambient air (21°C), the time it takes to reach the crystallization temperature, after melting, is significantly shorter for the C58 compared to the C28. By choosing the C58 instead of the C28, the experiments could be performed at a shorter time. A time plot, showing the crystallization time for the C58 can be found in appendix C.

## 5.5. Electrical Resistance Measurements

A fixed electrical current from a pre-set voltage source was allowed to pass through liquid PCM-samples during crystallization induced by ambient cooling (method further described in section 4.2.5). The residual current passing through the samples was measured and compared to the corresponding DSC curves for each material throughout crystallization. The results of three separate measurements for PEG1000 is seen in figure 26.
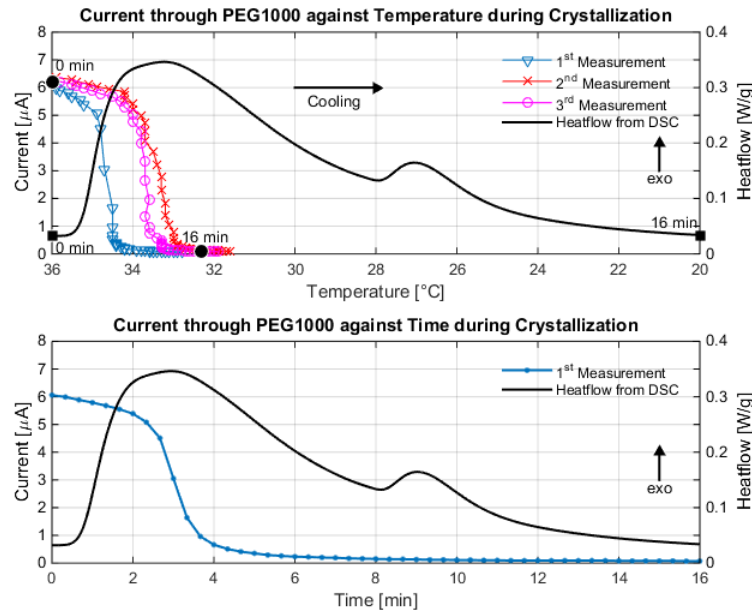
***Figure 26:*** *This figure shows the results from three electrical measurements of PEG1000 plotted against both the temperature (upper panel) and the time (bottom panel).*

The residual current drops linearly during cooling as PEG1000 is in its liquid state, i.e. above 35°C. A rapid drop in residual current is observed as the polymer undergoes crystallization between 33-35 °C (seen in the upper panel of figure 26). Assuming that the drop in residual current (at approximately 35 °C) is solely a result of the crystallization, these results suggests that the residual current passing through PEG1000 is directly related to the degree of crystallinity of the polymer. By measuring the residual current at any given temperature, it is possible to quantify the SOC. For instance, if the current is above 6 $\mu A$, PEG1000 is in its liquid state (or 100% "loaded" in the terms of SOC). If the current is in between 0.5-6 $\mu A$, it is partly in liquid and partly in crystalline state (or between 0-100% in terms of SOC) depending on the value of the current. A value close to 6 $\mu A$ means more liquid than crystalline, similarily a value close to 0.5 $\mu A$ means more crystalline than liquid. Additionally, if the current is in between 0-0.5 $\mu A$, PEG1000 is mostly in crystalline state (or fully "discharged" in terms of SOC). The same behavior during crystallization as observed for PEG1000 is also seen for PEG1500 in figure 27.
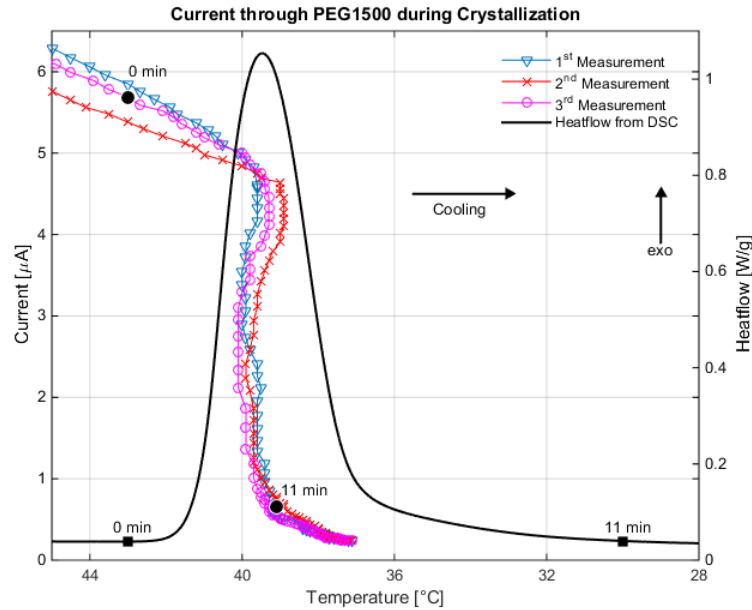
***Figure 27:*** *This figure shows the results from three electrical measurements of PEG1500 plotted against the temperature.*

The residual current drops linearly during cooling as PEG1500 is in its liquid state, i.e. above 40°C. A rapid drop in residual current is observed as the polymer undergoes crystallization, dropping from 5µA and approaches zero around 40 °C. Close to complete crystallization is achieved 11 minutes into the experiment and a corresponding time plot for PEG1500 can be found in appendix D. As the degree of crystallinity increases, so does the electrical resistance of the material, resulting in a drop in residual current passing through the sample according to Ohm's law (see equation *ix*). This method seems to work well for determination of the crystallinity of the polymers. However, this is not the case for erythritol, which can be seen in figure 28.
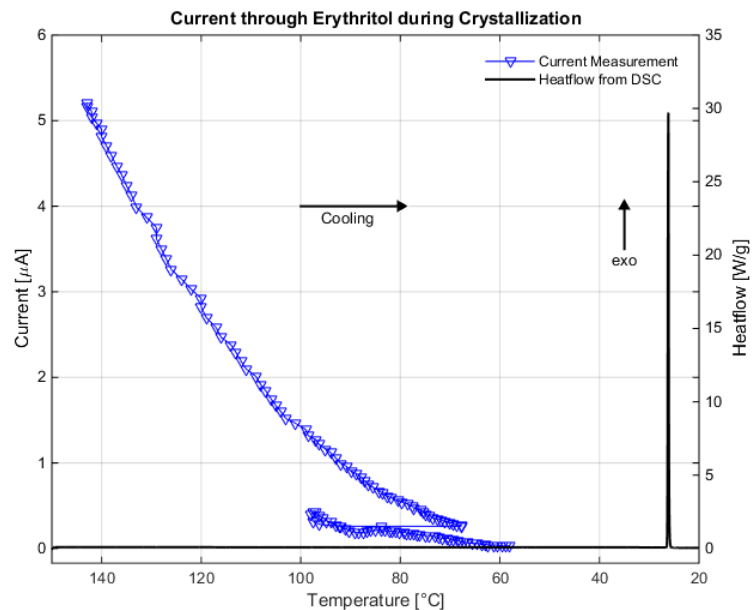


***Figure 28:*** *This figure shows the results from a single electrical measurement performed on erythritol plotted against the temperature.*

Similar to the polymers, the residual current drops continuously for erythritol during cooling as it is in its liquid state, i.e. above 70 °C. The crystallization occurs at approximately 70 °C, which is above the crystallization temperature indicated by the DSC curve at 27.6 °C. The large amount of LH released during the crystallization raises the sample temperature from 70 to 95 °C, which can be seen in figure 28. The residual current then continues to drop and approaches zero. The significant difference between the crystallization temperature indicated by the DSC curve (27.6 °C) and the one observed during this experiment (at approximately 70 °C), may again have to do with the big difference in sample volumes between the different techniques (only a few micro liters in the DSC compared to 40-50 mililiters for the electrical resistance measurements). The sample volume is directly realted to the degree of subcooling for certain PCM types, e.g. erythritol according to Hayashi et al. (26), as mentioned in section 5.4. The crystallization may also have been induced earlier during the electrical resistance measurement either through nucleation caused by impurities such as dust from the surrounding air or by the current supplied from the voltage source. Nevertheless, no observable relation can be seen between the residual current and the degree of crystallinity for erythritol.

Electrical resistance measurements were also performed on the salt hydrate C28, where another problem appeared. A blue/green-colored solid substance started to form on the katode surface, seen in figure 29. The electrically charged ions within the material were strongly affected by the induced current through the material, resulting in an undesired ion movement towards the electrodes. The zinc coating surrounding the copper katode dissolved into the sample solution as zinc ions, exposing the copper core. Simultaneously the free ions, belived to be sulphate ions (no laboratory validation), in the C28 moved towards the katode forming a coating of copper sulphate on the electrode surface. As a result of this undesired ion movement the chemical composition of the salt hydrate was changed which questions the obtained results.
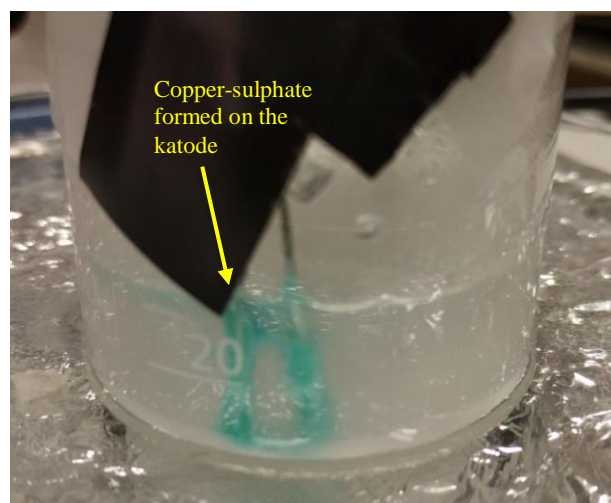


*Figure 29: This figure shows a photo of the blue/green copper sulphate forming on the katode surface when performing electrical resistance measurement on the C28.*

Additionally a final measurement was performed on xylitol investigating whether or not it is possible to extort crystallization by supplying an electric current. The sample was melted and cooled down to 25 °C by the ambient air without indication

of an occurring crystallization at any time. The xylitol remained in its amorphous metastable state throughout the experiment. A figure showing these results can be found in appendix D.

### 5.6. Dielectric Measurement

The conductivity was measured using dielectric spectroscopy according to the method described in section 4.2.6. One PCM from each of the investigated PCM types were tested; PEG1000, erythritol and C28. The PCMs were pre-melted prior to the measurements in order to ensure good dispersion of the sample inside the sample cell as well as enabling a satisfactory contact area between the sample and the electrodes. The conductivity was measured both during melting and crystallization for the frequencies 40, 50 and 60 Hz. Due to the occurrence of artifacts (measurement disturbances) throughout these experiments caused by formation of cracks in the PCM samples during crystallization, some deviating data points have been removed when compiling the results for PEG1000 and erythritol. The unchanged results, before removal of the artifacts, for these measurements can be found in appendix E. The results from the measurement on PEG1000, after removal of the artifacts can be seen in figure 30.
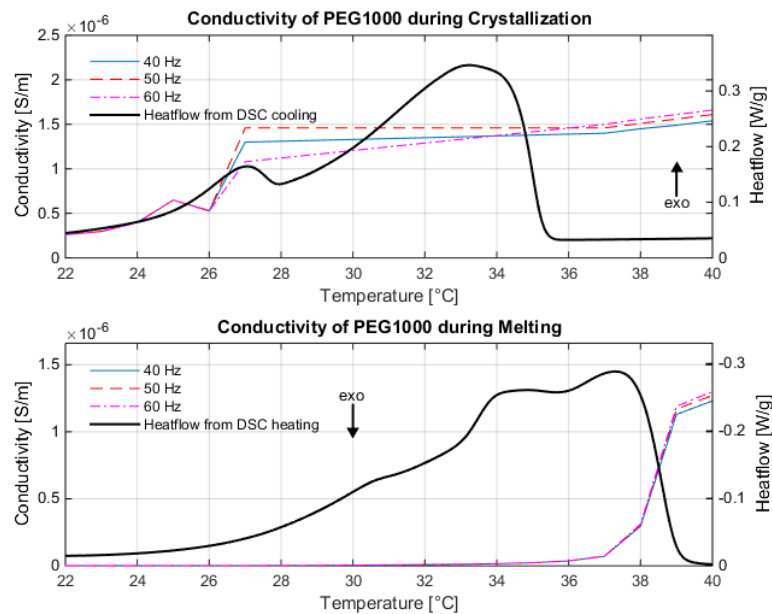


***Figure 30***: *This figure shows the changes in conductivity of PEG1000 during crystallization (upper panel) and melting (bottom panel) for the frequencies 40, 50 and 60 Hz. The conductivity decreases slightly during cooling, until reaching 27 °C, where a drop is observed. The conductivity shows a significant increase after being heated above 36 °C during the melting.*

The conductivity of PEG1000 decreases slightly during cooling between 27-40 °C and then drops down, as the polymer is being cooled below 27 °C (seen in the upper panel of figure 30). The drop in conductivity at 27 °C is an indication of an occurring crystallization. The melting curve (bottom panel in figure 30) shows a significant increase in conductivity as the sample starts to melt, after being heated above 36 °C. This increase in conductivity during the melting, shows potential to be related to the degree of crystallinity of PEG1000 and thereby also the SOC (since the conductivity increases from approximately 0.05 $S/m$, in its solid state to

approximately 1.6 $S/m$, in its liquid state). In general, the conductivity is seen to be slightly higher as PEG1000 is in its liquid state (above 39 °C) compared to its solid state. This is also the case for erythritol, which can be seen in figure 31.
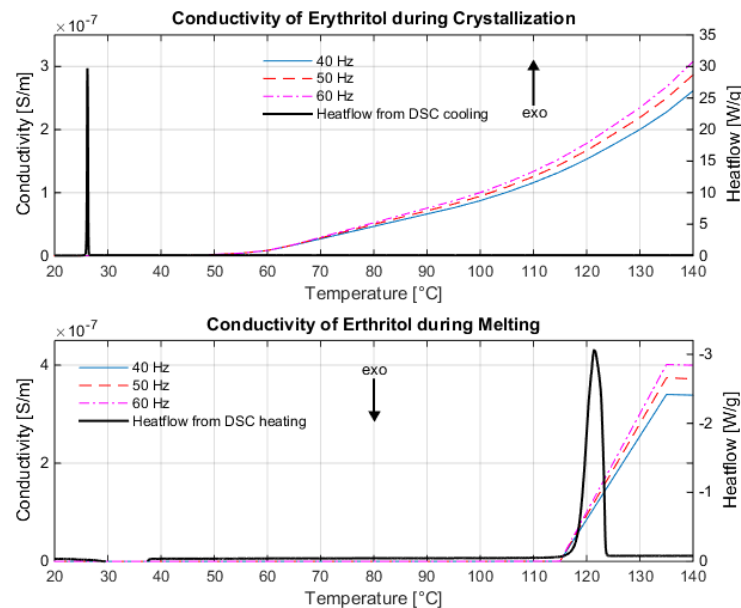


***Figure 31***: *This figure shows the changes in conductivity of erythritol during crystallization (upper panel) and melting (bottom panel) for the frequencies 40, 50 and 60 Hz. A drop in conductivity is visible during the crystallization between 55-140 °C and an increase in conductivity is observed during the melting at 115 °C, before it levels out.*

The conductivity of erythritol is observed to be higher in its liquid state (above 120 °C) compared to its solid state. The increase in conductivity after being heated above 115 °C (seen in the bottom panel of figure 31) coincides with the melting peak from the DSC reasonably well. However, no change in conductivity is observed in the proximity of the crystallization peak indicated by the DSC at 27.6 °C (seen in the upper panel of figure 31). Furthermore, the continuous drop in conductivity observed throughout the cooling, shows no indication of being related to an occurring crystallization at any point of the measurement. The conductivity only drops as a result of a lower temperature. This behavior was also observed during the electrical resistance measurement performed on erythritol, where the residual current only dropped as a result of decrease in temperature (seen in figure 28, section 5.5). Figure 32 shows the results from the measurement performed on the salt hydrate C28 which demonstrates a different behavior.
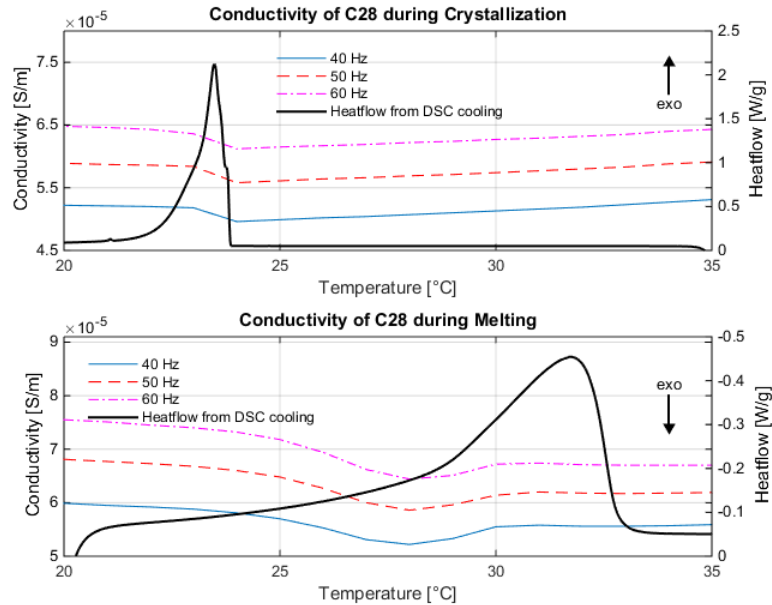
***Figure 32***: *This figure shows the changes in conductivity of C28 during crystallization (upper panel) and melting (bottom panel) for the frequencies 40, 50 and 60 Hz. A slight increase is visible during the crystallization between 23-24 °C and the conductivity seems to drop to a minimum value at approximately 28 °C during the melting.*

In contrast to PEG1000 and erythritol, the C28 shows a higher conductivity in its solid state (below 23 °C) compared to its liquid state. There is also a distinct difference in conductivity between the different frequencies. The conductivity is strictly higher for higher frequencies but follows the same pattern during a temperature ramp. During the crystallization (upper panel of figure 32) the conductivity is seen to slowly decrease as the temperature gets lower. At approximately 24 °C a small increase in conductivity is observed for all frequencies. This increase in conductivity coincides very well with the crystallization temperature indicated by the DSC curve at 24.1 °C. Throughout the melting (bottom panel of figure 32) the conductivity decreases upon heating, reaching a minimum value at approximately 28°C for all frequencies. The conductivity then increases slightly before it levels out above 30 °C. These minimum values at 28 °C are fairly close to the melting temperature of the C28 at 31.6 °C and suggests a possible relation between the conductivity and the degree of crystallinity for C28. However, the fact that the material shows a higher conductivity in its solid state compared to its liquid state is really unexpected. No previous studies verifying these results have been found. Normally a material shows a higher conductivity in its liquid state since the molecules (or ions) are able to move more freely compared to when they are in a fixed crystalline structure. A possible explanation to these results is that volatile compounds within the C28 may have evaporated from the sample during the long measurement time (10 hours), affecting the chemical composition of the C28 and thereby its properties. Additionally the electricity supplied by the dielectric equipment induces undesired ion movement within the sample (similar to the electrical resistance measurement, seen in figure 29, section 5.5), which also affects the chemical composition of the C28.

# 6. Summary and Concluding Discussion

## 6.1.    Comparison and Evaluation of the Different Techniques

The physical and chemical properties of PCMs varies differently during phase transitions depending on the PCM type. This provides a great challenge when it comes to utilizing these changes to visualize the SOC. Based on the results from this study, it is hard to select a single measuring technique that can visualize the SOC for all types of PCMs. A method that works well to determine the SOC for polymers does not necessarily work for salt hydrates and vice versa. This means that the measuring technique has to be selected to match the specific PCM type. Additionally, different methods have shown varying results for the same material, which can be seen in figure 33 for PEG1000. After normalization of the results they can be compared both to the DSC curve and to each other. It is seen that all of the techniques indicates a property change in the region of crystallization, but to a varying degree and with various accuracy compared to the DSC curve. The viscosity and density measurements shows a property drop, close to the crystallization temperature, as a result of equipment limitations and can therefore not be related to the SOC. The light transmittance and the electrical resistance measurements shows a similar property drop at approximately 35°C which is really close to the crystallization temperature. These techniques could possibly be used for quantification of the SOC for PEG1000 since no other peaks or drops are observed. The conductivity also shows a drop, but at a lower temperature compared to the other techniques.
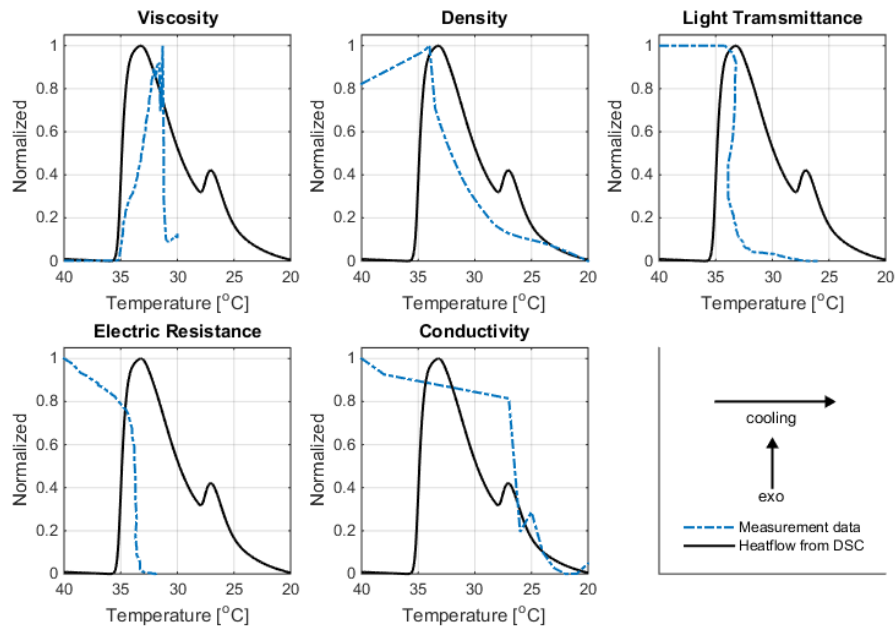


***Figure 33:*** *This figure shows a comparison of all methods evaluated throughout this study for PEG1000 during crystallization (all data have been normalized).*

Throughout this project, focus has been to visualizing the SOC during crystallization rather than melting. The reasons for this is partly that it is easier to achieve uniform cooling compared to uniform heating by cooling the PCM with the ambient air instead of using different heating devices. Furthermore, since the

primary way of measuring the temperature of the PCMs has been to use an IR camera, more reliable data could be obtained if focusing on the crystallization instead of the melting, to minimize disturbances from a heat source. However, to use an IR camera on the sample container to determine the sample temperature may not have been the best solution when it comes to reliability. Ideally it would be better to use a thermometer or temperature sensors inside the sample container to get more accurate temperature data. The reasons for why such equipment was not used for these experiments is due to the lack of space within the cuvette for the optical measurements and also for possible interferences with the measurement results (such as impurities on the equipment). To use DSC data as a reference to verify the accuracy and reliability of other measurement techniques has worked well in most cases. One exception is for erythritol where DSC analysis results in a substantial subcooling (of approximately 100 °C) which was not observed for any other techniques to the same extent. This high degree of subcooling during DSC analysis of erythritol has been seen in previous studies as well. A more suitable reference such as T-history could have been used instead to get a more suitable reference to the measurements performed on erythritol.

The optical light transmittance measurements have shown good and consistent results for PCMs that changes from a clear transparent liquid into an opaque solid during crystallization. The amount of light able to pass through the sample is seen to be directly related to the degree of crystallization for several PCM types. Rheological property changes such as viscosity and density have been harder to correlate to the SOC. Peaks in viscosity and density were observed in the close proximity of the crystallization temperature for the polymeric PCMs. However due to apparatus limitations, when it comes to heating possibilities or material sensitiveness, results could not be generated for all types of PCMs using these methods. The electrical resistance method demands a high level of resolution on the detection equipment to be able to measure the relatively low level of residual current able to pass through the PCM sample. As a result of the high electrical resistance shown by the majority of the investigated PCMs only a small fraction of the current is able to pass through the sample (a few ppm). This method has shown different results depending on the PCM type. A clear drop in residual current is seen for the PEGs during crystallization, while no observable relation between the drop in residual current and the degree of crystallinity can be seen for erythritol. Furthermore, this method cannot be used for PCMs consisting of electrically charged ions since the generated current induces an undesirable ion movement towards the electrodes.

## 6.2.    Suggested Practical Implementations

When it comes to commercial suitability, most of the investigated techniques could be modified to operate in a building environment. The optical method, that utilizes transparency changes of a PCM during phase transition and correlates it to the degree of crystallization, shows good potential to be implemented commercially. No previous experimental studies investigating large scale implementation of this technique have been found. However, we believe it is possible to test this technique in larger scale by using optical fibers. By connecting optical fibers between a light source and the enveloped PCM and between the PCM and a light sensor, the light

transmittance of the material can be measured directly. A sketch of a possible setup can be seen in figure 34.
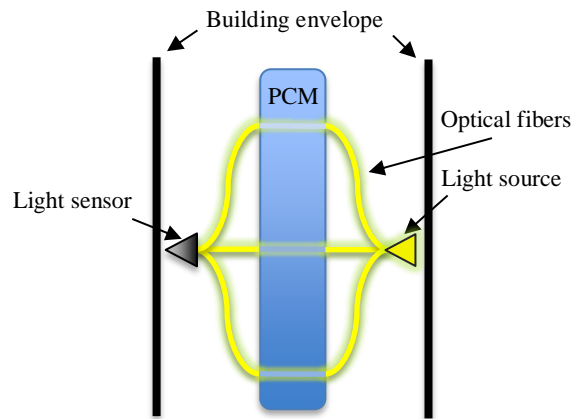


***Figure 34:*** *This figure shows a proposed large scale implementation design of the optical light transmittance technique (the optical fibers does not go through the PCM container).*

For this implementation, the PCM has to be contained in envelopes and then integrated into the building. Applications where the PCM is encapsulated in other materials such as gypsum or concrete will not work for this technique, since the light transmittance would be very hard to measure (the same is true for techniques that measures rheological properties or volumetric change). This method requires that the PCM envelop can be penetrated by light in some way, either by using a completely transparent envelop or by having transparent zones on the envelope surface through which light can pass through. In addition, this method only works for PCMs that shows a distinct difference in light transmittance between their liquid and solid state. Based on the results presented in this report it is possible to measure the light transmittance during crystallization for a specific type of PCM and correlate the results to the heat flow variations obtained from a DSC. By doing this it is possible to get a good estimation of what level of light transmittance that corresponds to a certain degree of the SOC of the material. Light sensors as well as optical fibers are considered relatively cheap (compared to the material cost), which is good from an economical point of view.

The rheological methods measuring the viscosity or density differences during crystallization and melting, will be harder to implement in a commercial manner. These techniques requires some kind of forced movement upon the PCM inside a closed container, which could be hard to design practically. An alternative is to utilize the volumetric change of the material that occurs as the PCM undergoes phase transition (described in section 3.2.1). Assuming that the PCM is encapsulated in a closed container, a difference in internal pressure within the container will arise during phase transitions, as a result of the volumetric change. An illustration of a possible setup for this technique is seen in figure 35.
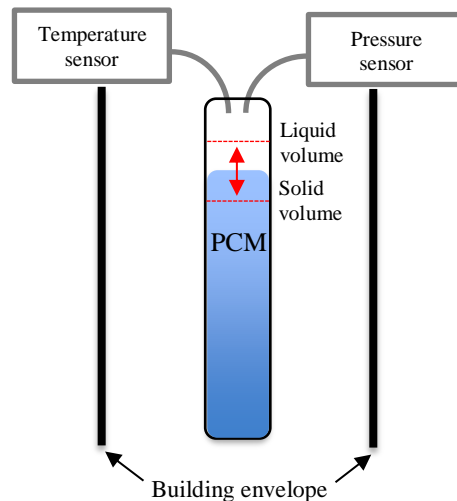
*Figure 35: This figure shows a proposed large scale implementation design of the volumetric change technique using pressure and temperature sensors.*

By measuring these changes using pressure sensors, it is possible to correlate them to the degree of crystallization of the material. This technique requires a PCM that shows a relatively large difference in volume between its liquid and solid state, such as paraffins. The technique has been tested experimentally by Steinmaurer et al. (7) showing positive results, however no verification of these results has been made in this study. With regards to the economical aspect of this method it shows great potential, since neither temperature nor pressure sensors are particularly expensive.

The different types of electrical measuring techniques described in this report could also possibly be used commercially. The changes in electrical resistance of a PCM integrated in a building could be measured in a similar fashion as performed in this project. By establishing a source of voltage between two electrodes (or plates) integrated inside a closed PCM container, the residual current could be measured continuously throughout a phase transition using an ampere meter. Since the residual current is related to the electrical resistance of the material, according to Ohm's law (see equation $ix$), it is possible to calculate the electrical resistance solely by measuring the residual current (assuming that the voltage and ingoing current are known and constant). This technique may also work for applications were the PCM is encapsulated within a porous carrier material if using plates instead of electrodes, in direct contact with the material, see figure 36.
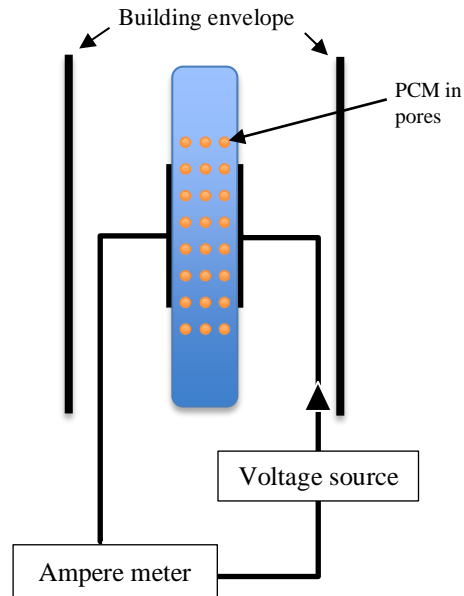
***Figure 36:*** *This figure shows a proposed large scale implementation design of the electrical resistance technique using plates since the PCM is integrated in pores.*

Based on results seen in this report, the electrical resistance is only correlatable to the SOC for the PEGs and not for sugar alcohols nor salt hydrates. This limits the usage potential of PCMs for utilization of this technique. However, no expensive equipment is needed to implement this technique commercially.

# 7. Conclusion

This Master´s thesis aimed to answer two research questions:

1. What are the most suitable performance indicators to visualize the SOC in PCMs based on polymers, sugar alcohols and salt hydrates?

2. How could the performance indicator(s) be implemented effectively to visualize the SOC in the PCM for a large scale building application?

This study has evaluated different techniques for SOC measurements in PCMs and shown that it is possible to indirectly detect phase transitions without using thermal methods. Certain PCM types needs specific sample preparation and measuring conditions in order for reliable results to be obtained. The salt hydrates have been exceptionally hard to evaluate due to the release of volatile components when being exposed to the surrounding air.

One method that has shown promising results for all of the investigated PCMs is the optical light transmittance method. The light transmittance has shown to be indirectly related to the SOC according to the experimental results presented in this study and even making it possible to quantify. A proposed design to make this method commercially suitable, both practically and economically, has been suggested, although not tested experimentally. Furthermore, the electrical resistance technique has seen to work satisfactory for quantitative analysis of the SOC for the investigated PEGs. The rheological methods (viscosity and density) have indicated property changes during the phase transitions but these changes cannot be correlated to the SOC in an obvious way. The dielectric method also points to changes in conductivity during the phase transitions for the examined PCMs, however, quantitative determination of the SOC based on this method has shown limited potential. In table 2, a complete summary of the performance for the investigated techniques is presented. A green checkmark means that the technique is able to detect either phase transitions (PT) or the state of charge (SOC), whereas a red cross means that the technique fails to provide such results. N/A means that the technique is unable to provide any results due to equipment limitations. Question marks are used when the results are inconclusive.

***Table 2:** This table shows a summary of the performance for the investigated measurement techniques when it comes to visualizing phase transitions and/or the SOC.*

| | Viscosity | | Density | | Electrical Resistance | | Dielectric | | Light Transmittance | |
|---|---|---|---|---|---|---|---|---|---|---|
| | PT | SOC | PT | SOC | PT | SOC | PT | SOC | PT | SOC |
| **Polymers** | ✓ | ✗ | ✓ | ✗ | ✓ | ✓ | ✓ | ? | ✓ | ✓ |
| **Sugar Alcohols** | N/A | N/A | N/A | N/A | ✗ | ✗ | ✓ | ? | ✓ | ✓ |
| **Salt Hydrates** | ✓ | ✗ | N/A | N/A | ✗ | ✗ | ✓ | ? | ✓ | ✓ |

PT – Technique indicates phase transition     N/A – Not applicable
SOC – Technique is able to detect state of charge     ? – Questionable results

To summarize, the light transmittance method, electrical resistance method and possibly the dielectric method can be used to determine the SOC for PEGs (i.e. polymers). Only the optical light transmittance method has shown positive results for SOC determination for sugar alcohols (erythritol) and salt hydrates (C58).

Regarding commercial suitability, different techniques could be used depending on how the PCM is integrated into the building. For technical solutions were the PCM is encapsulated in a closed container, the optical method is a suitable performance indicator. For other solutions where the PCM is integrated in various porous carrier materials, electrical methods could be used instead, measuring changes in either electrical resistance or conductivity.

# 8. Further Studies

This study has investigated different methods to visualize the SOC in PCMs and offers a foundation from where to continue. First of all, more PCMs needs to be tested to verify if the methods can be used for a broader variety of PCMs. One particular type of interest is the salt hydrates which are hard to evaluate if the composition is unknown (as in this study), since the experimental results are hard to predict without testing, resulting in a "trial and error" approach. But if the composition is known, it will be easier to create experiments around the material and thereby increasing the chances of selecting a method that is suitable for that specific PCM type. Other PCM types to evaluate further are the polymers and paraffins, which have many different compounds that can be of interest and where this study has only investigated PEGs.

Furthermore it is of interest to measure the SOC during melting of the PCM to get results both from the crystallization and the melting. By comparing such results it would be easier to verify reliability, accuracy and consistency of the investigated techniques. To be able to do that, proper heating equipment (that heats the material from all directions) is needed to get valid results.

The method that relates the SOC to the volumetric change of a PCM during phase transitions (by measuring the pressure differences inside a closed container) would be of great interest to test experimentally. This technique utilizes simple and inexpensive equipment and has the potential to determine the SOC for a variety of different PCM types. This requires an integrated temperature and pressure sensor within in a hermetically sealed PCM container and could theoretically be used for any PCM that shows a large volumetric difference between its liquid and solid state.

Additionally, to actually build small models with the proposed designs from section 6.2, to see if the methods could be applied to a "real" building envelope, seems like a natural continuation on this project.

# 9. References

1. **U.S. Energy Information Administration.** eia.gov. *How much energy is consumed in the world by each sector?* [Online] 2016. [Cited: January 19, 2016.] http://www.eia.gov/tools/faqs/faq.cfm?id=447&t=1.

2. *Sectorial trends in global energy use and greenhouse gas emissions.* **de Ia Rue du Can, S. and Prive, L.** s.l. : Elsevier, 2008, Energy Policy, Vol. 36, pp. 1386-1403.

3. *Phase change materials and products for building applications: A state-of-the-art review and future research opportunities.* **Edsjø Kalnæs, S. and Jelle, B-P.** s.l. : Elsevier, 2015, Energy and Buildings, Vol. 94, pp. 150-176.

4. *PCM thermal energy storage in buildings: experimantal study and applications.* **Guario, F., et al.** s.l. : Elsevier, 2015, Energy Procedia, Vol. 70, pp. 219-228.

5. *Application of PCM thermal energy storage system to reduce energy consumption.* **Jeon, J., et al.** s.l. : Akadémiai Kiadó, 2012, Journal of Thermal Analysis and Calorimetry, Vol. 111, pp. 279-288.

6. *DHFMA Method for Dynamic Thermal Propert Measurement of PCM-integrated Building Materials.* **Shukla, N. and Kosny, J.** 2, s.l. : Springer International Publishing AG, 2015, Current Sustainable/Renewable Energy Reports, Vol. 2, pp. 41-46. s40518-015-0025-x.

7. *Development of sensors for measuring the enthalpy of PCM storage system.* **Steinmaurer, G., Krupa, M. and Kefer, P.** s.l. : Elsevier, Energy Procedia, Vol. 48, pp. 440-446.

8. *Thermal energy savings in buildings with PCM-enhanced envelope: Influence of occupancy pattern and ventilation.* **Diaconu, B. M.** s.l. : Elsevier, 2011, Energy and Buildings, Vol. 43, pp. 101-107.

9. **Elliott, J. R. and Lira, C. T.** *Introductory chemical engineering thermodynamics.* 2. Upper Saddle River, NJ : Pearson, 1999.

10. *Phase Change MAterials for Building Applications: A state-of-the-art review.* **Baetens, R., Jelle, B-P. and Gustavsen, A.** s.l. : Elsevier, 2010, Energy and Buildings, Vol. 42, pp. 1361-1368.

11. **Schaschke, C.** *A Dictionary of Chemical Engineering.* s.l. : Oxford University Press, 2014.

12. *Eutectic Mixtures of Sugar Alcoholes for Thermal Energy Storage in the 50-90 C Temperature Range.* **Diarce, G., et al.** s.l. : Elsevier, 2014, Solar Energy & Solar Cells, Vol. 134, pp. 215-226.

13. *Manipulation of phase transition temperatures and supercooling of sugar alcohols based Phase Change Materials (PCMs) by urea.* **Göhl, J., et al.** 2016.

14. **Engineering.com.** Thermal Conductivity. *www.engineering.com.* [Online] [Cited: 05 30, 2016.] http://www.engineering.com/Library/ArticlesPage/tabid/85/ArticleID/152/categoryId/11/Thermal-Conductivity.aspx.

15. *Enhanced thermal conductivity of PEG/diatomite shape-stabilized phase change materials with Ag nanoparticles forthermal energy storage.* **Qian, T., et al.** 2015, Journal of Materials Chemistry A, Vol. 3, pp. 8526-8536.

16. *Enhanced thermal conductivity and thermal performance of form-stable composite phase change materials by using B-Aluminum nitride.* **Wang, W., et al.** s.l. : Elsevier, 2009, Applied Energy, Vol. 86, pp. 1196-1200.

17. *Enhanced comprehensive per-formance of polyethylene glycol based phase change material with hybrid graphene nanomaterials for thermal energy storage.* **Guo-Qiang, Q., et al.** s.l. : Elsewier, 2015, Carbon, Vol. 88, pp. 196-205.

18. *A review on energy conservation in building applications with thermal storage by latent heat using phase change materials.* **Khudhair, A. M. and Farid, M. M.** s.l. : Elsevier, 2004, Energy Conversion and Management, Vol. 45, pp. 263-275.

19. *Determination of the enthalpy of PCM as a function of temperature using a heat-flux DSC-A study of different measurement procedures and their accuracy.* **Castellón, C, et al.** s.l. : Wiley InterScience, 2008, International Journal of Energy Research, Vol. 32, pp. 1258-1265.

20. **Jansson, H.** *Dynamical properties of interfacial water and its role for biomolecular dynamics.* s.l. : Chalmers University of Technology, 2006. 91-7291-864-0.

21. *Performance characterization of PCM impregnated gypsum board for building applicaions.* **Shukla, N., Fallahi, A. and Kosny, J.** s.l. : Elsevier, 2012, Energy Procedia, Vol. 30, pp. 370-379.

22. **Mehling, H. and Cabeza, L. F.** *Heat and cold storage with PCM.* Berlin : Springer, 2008. 978-3-540-68557-9.

23. **Johansson, P., Sasic Kalagasidis, A. and Jansson, H.** Investigating PCM activation using transient plane source method. 2015.

24. **Bruno, F, et al.** *Advances in THermal Energy Storage System.* s.l. : Woodhead Publishing, 2014.

25. **Rheosys LLC.** A Basic Introduction to Viscometers & Viscometry. *http://www.rheosys.com.* [Online] [Cited: February 3, 2016.] http://www.rheosys.com/intro.html.

26. **Novocontrol Technologies.** Dielectric Spectroscopy, Conductivity Spectroscopy, and Electrochemical Impedance Spectroscopy. [Online] [Citat: den 23 03 2016.] www.novocontrol.de/html/intro_overview.htm.

27. —. Applications. [Online] [Citat: den 23 03 2016.] www.novocontrol.de/html/intro_appl.htm.

28. *Preparation of Microcapsules Containing Erythritol with Interfacial Polycondensation Reaction by Using the (W/O) Emulsion.* **Hayashi, Y., et al.** s.l. : Sientific Research, 2014, Journal of Encapsulation and Adsorption Sciences, Vol. 4, pp. 132-141.

29. *Standardization of PCM Charachterization via DSC.* **Cabeza, L.F., o.a.** u.o. : Research Gate, 2015.

30. **Anton-Paar.** Laboratory Density and Concentration Meters. *www.anton-paar.com.* [Online] 2015. [Cited: February 4, 2016.] https://www.google.se/url?sa=t&rct=j&q=&esrc=s&source=web&cd=3&ved=0ahUKEwj7uKC0-d3KAhVBCiwKHYHSA_IQFggvMAI&url=http%3A%2F%2Fwww.anton-paar.com%2F%3FeID%3DdocumentsDownload%26document%3D3085%26L%3D6&usg=AFQjCNEisvCFrtOQvBWgGm8Y9edzb6JwRw&sig2=mKahViXM3rZC.

# List of Appendices

# Appendix A. DSC Reference for Studied PCMs

This appendix contains the calorimetric DSC data used as a reference to the other measurement techniques. The data were obtained using a METTLER TOLEDO DSC analyzer, with sample sizes in the range of 10-20 $\mu g$. From these results, reliable data for the melting and the crystallization enthalpies and temperatures could be obtained.
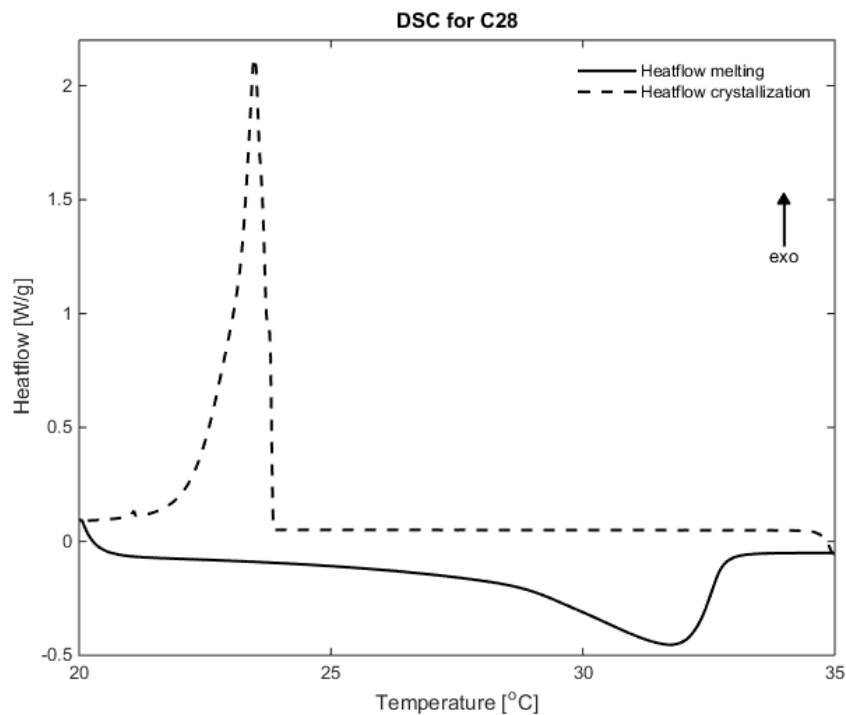


**Figure A-1:** *This figure shows the DSC-curve for C28 with a temperature gradient of* 1 ℃/min. *The crystallization temperature is indicated at 24.1 °C and the melting temperature is indicated at 31.6 °C.*
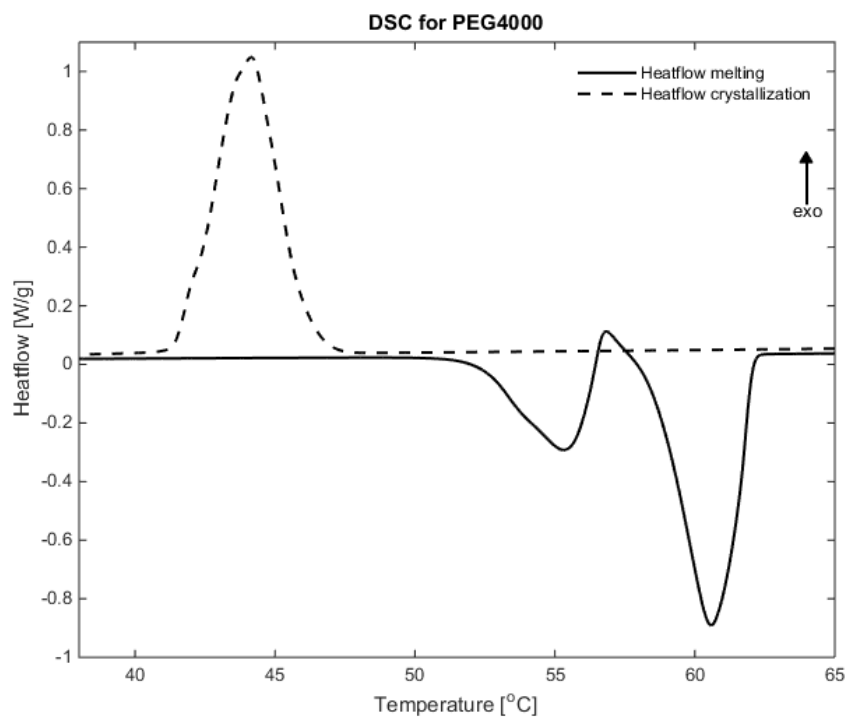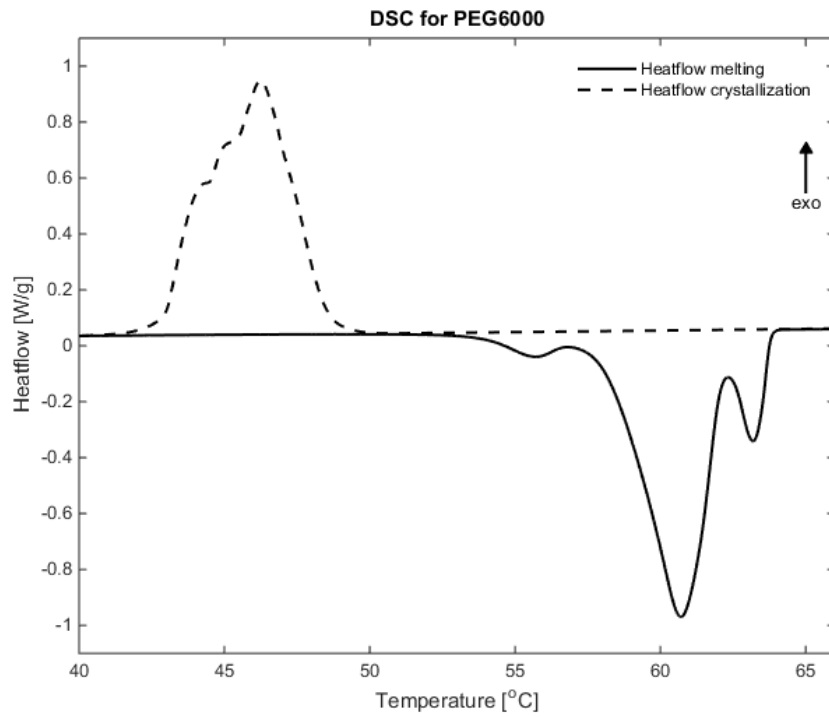
**DSC for C58**
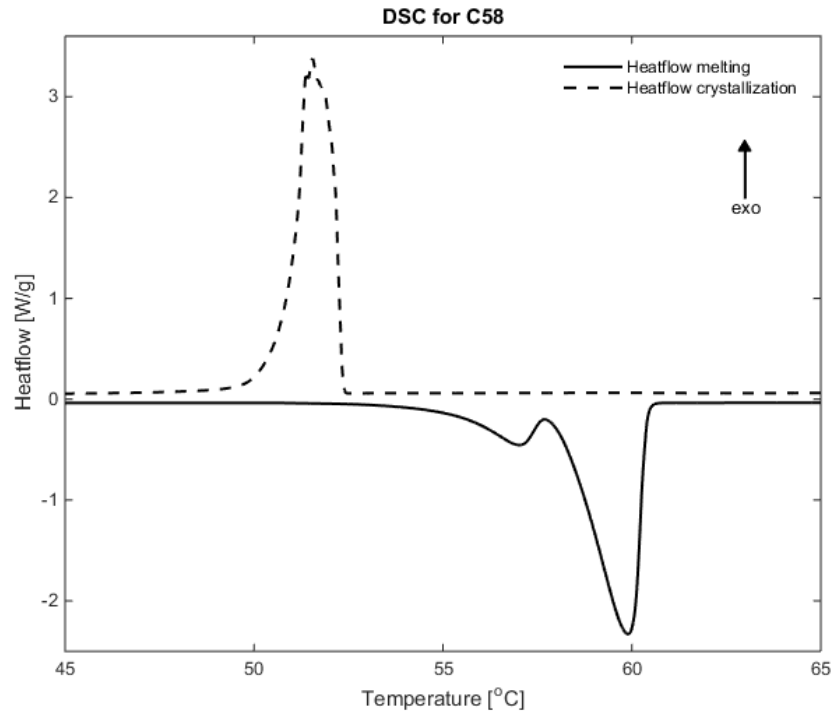
***Figure A-2:*** *This figure shows the DSC-curve for C58 with a temperature gradient of* $1 \; °C/min$*. The crystallization temperature is indicated at 52.4 °C and the melting temperature is indicated at 59.2 °C.*
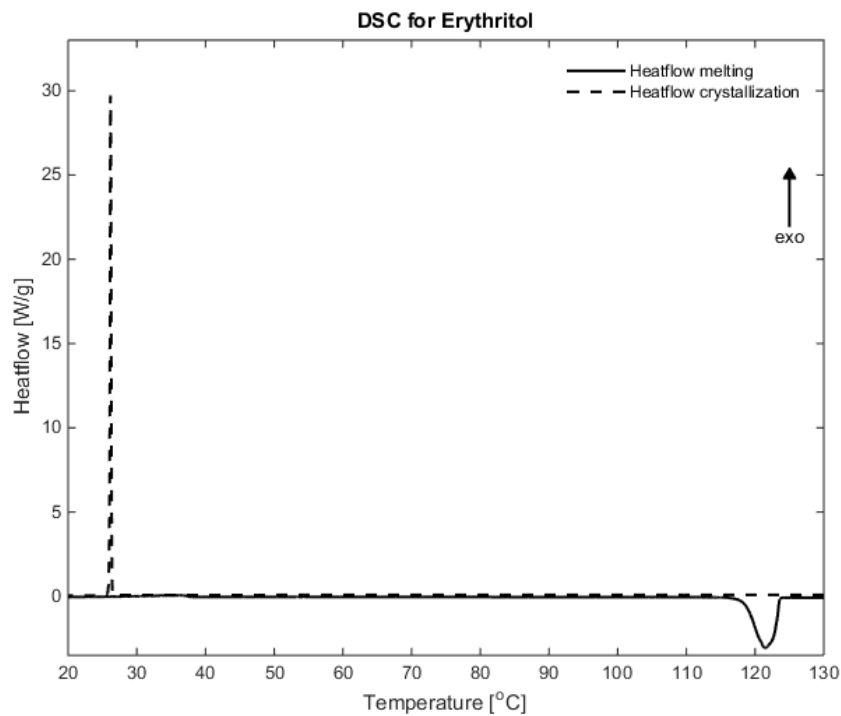


**DSC for Erythritol**

***Figure A-3:*** *This figure shows the DSC-curve for erythritol with a temperature gradient of* $1 \; °C/min$*. The crystallization temperature is indicated at 27.6 °C and the melting temperature is indicated at 119.6 °C.*
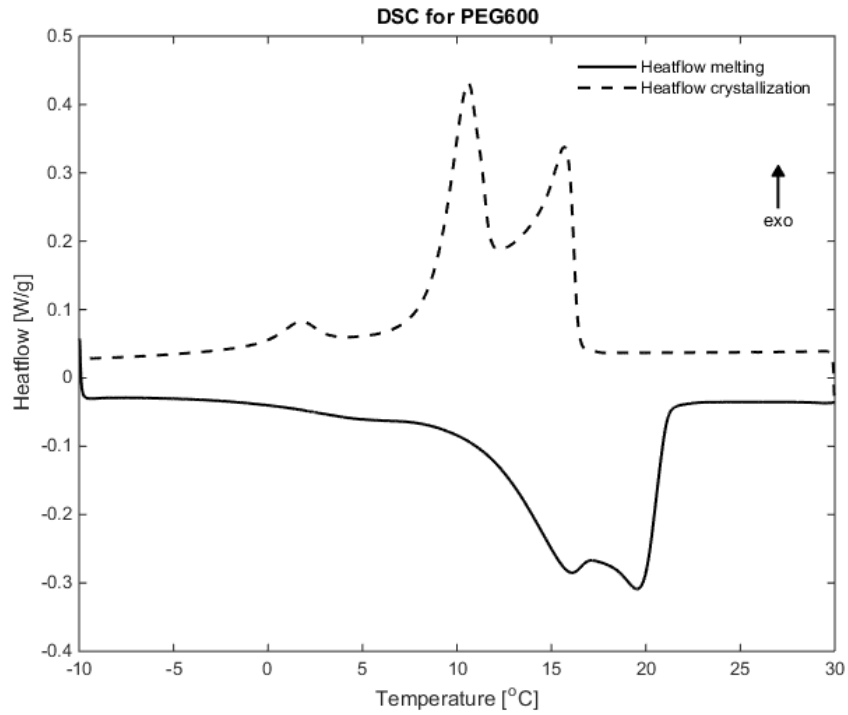
***Figure A-4:*** *This figure shows the DSC-curve for PEG600 with a temperature gradient of* 1 ℃/min. *The crystallization temperature is indicated at 10.6 °C and the melting temperature is indicated at 19.7 °C.*
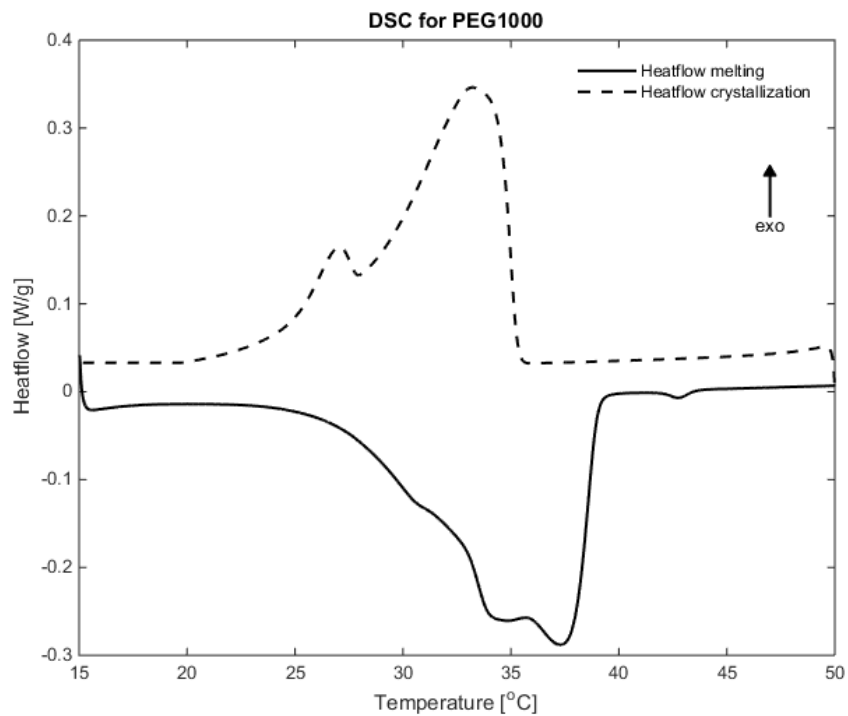


***Figure A-5:*** *This figure shows the DSC-curve for PEG1000 with a temperature gradient of* 1 ℃/min. *The crystallization temperature is indicated at 33.4 °C and the melting temperature is indicated at 37.1 °C.*
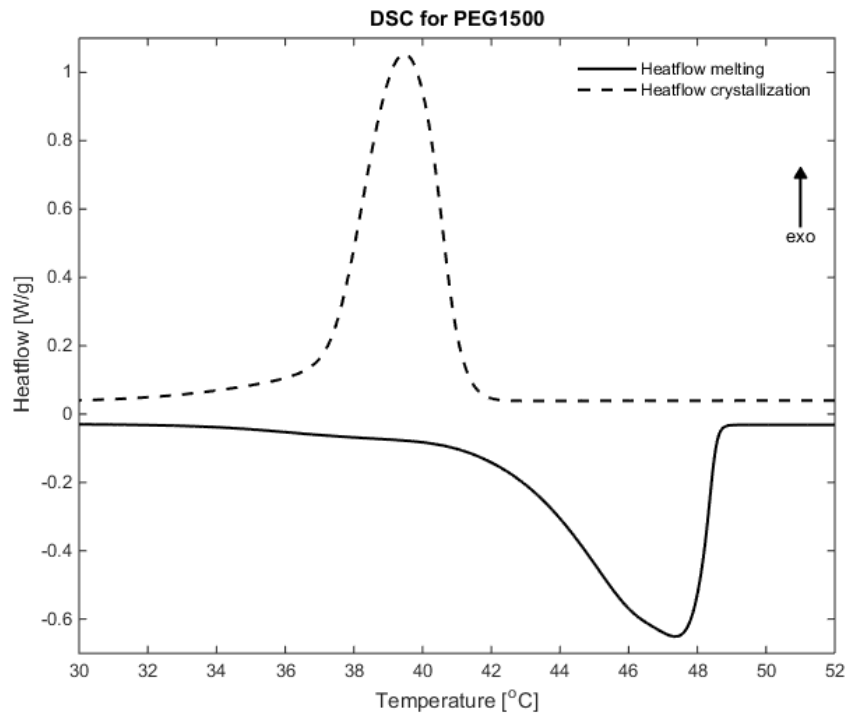
***Figure A-6:*** *This figure shows the DSC-curve for PEG1500 with a temperature gradient of* 1 ℃/min. *The crystallization temperature is indicated at 39.6 °C and the melting temperature is indicated at 47.6 °C.*



***Figure A-7:*** *This figure shows the DSC-curve for PEG4000 with a temperature gradient of* 1 ℃/min. *The crystallization temperature is indicated at 44.5 °C and the melting temperature is indicated at 60.9 °C.*

***Figure A-8:*** *This figure shows the DSC-curve for PEG6000 with a temperature gradient of* 1 ℃/min. *The crystallization temperature is indicated at 46.2 °C and the melting temperature is indicated at 61.1 °C.*

# Appendix B.    PEG1000 Light Transmittance Measurements

This appendix contains enlarged graphs from the light transmittance measurements for PEG1000. The results were obtained using the same method as described in section 4.2.4.
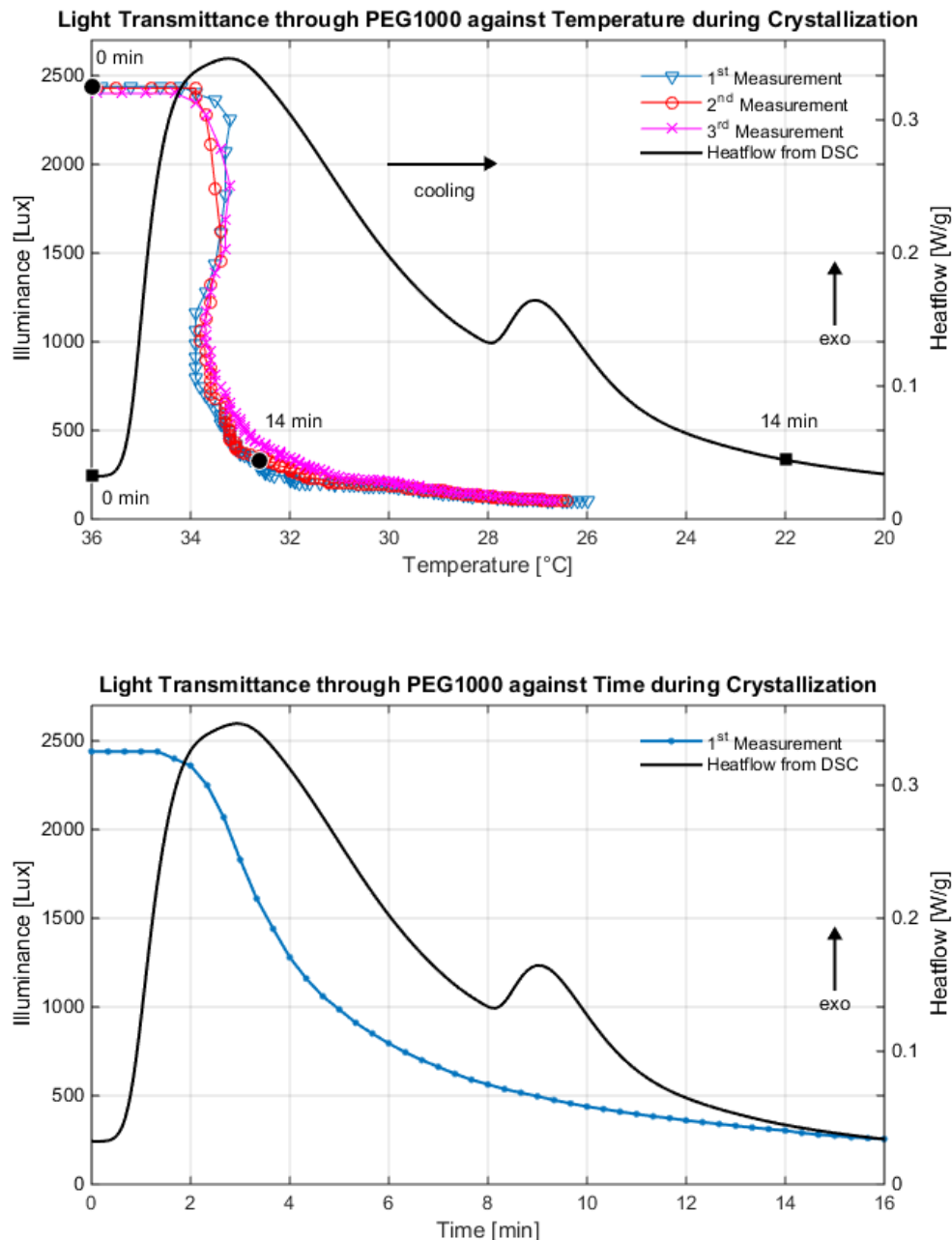




**Figure B-1:** *This figure shows the results from the light transmittance measurements for PEG1000, larger graphs. A complement to figure 22.*

# Appendix C.  Complementary Results to Light Transmittance Measurements

This appendix contains results from the light transmittance measurements for PEG4000 and PEG6000 as well as complementary time plots for all of the investigated PCMs. The results were obtained using the same method as described in section 4.2.4.
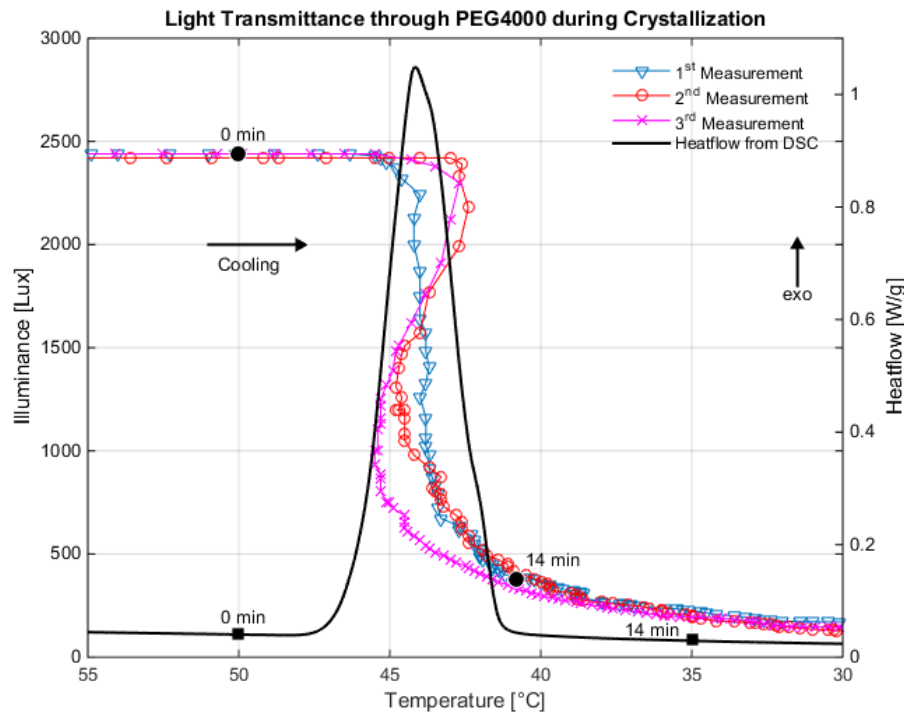


***Figure C-1*** *This figure shows the results from three light transmittance measurements of PEG4000 plotted against the temperature. The light transmittance remains constant at approximately 2450 lux as PEG4000 is in its liquid state, i.e. above 45 °C. As the crystallization starts, the light transmittance drops continuously and the LH released at this point results in an increase of the sample temperature. After 14 minutes approximately 95% of the polymer is in its crystalline state.*
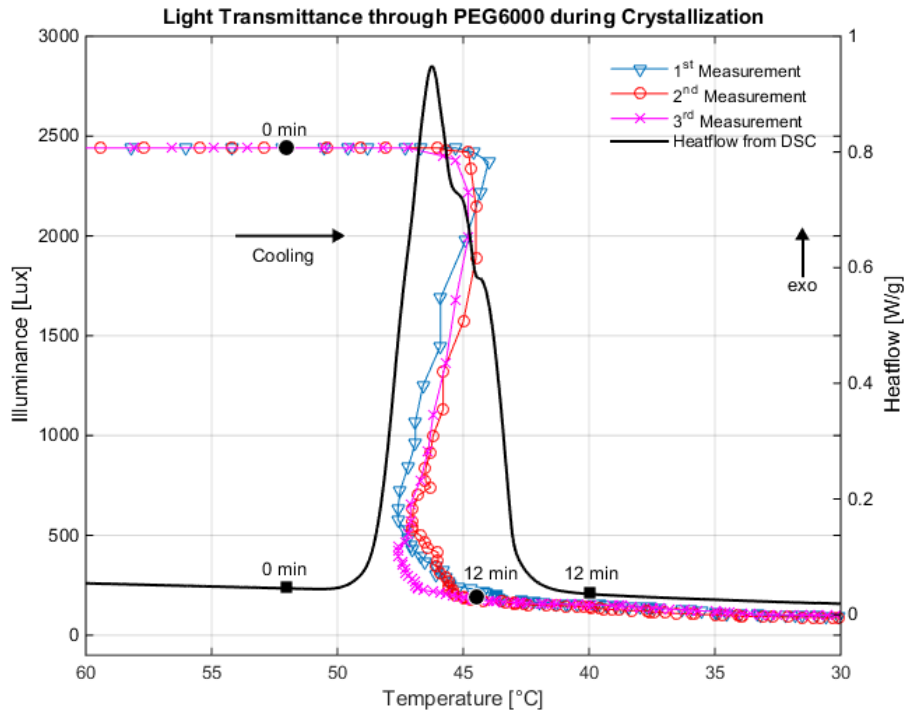
**Figure C-2:** *This figure shows the results from three light transmittance measurements of PEG6000 plotted against the temperature. The light transmittance remains constant at approximately 2450 lux as PEG6000 is in its liquid state, i.e. above 45 °C. As the crystallization starts, the light transmittance drops continuously and the LH released at this point results in an increase of the sample temperature. After 12 minutes approximately 95% of the polymer is in its crystalline state.*
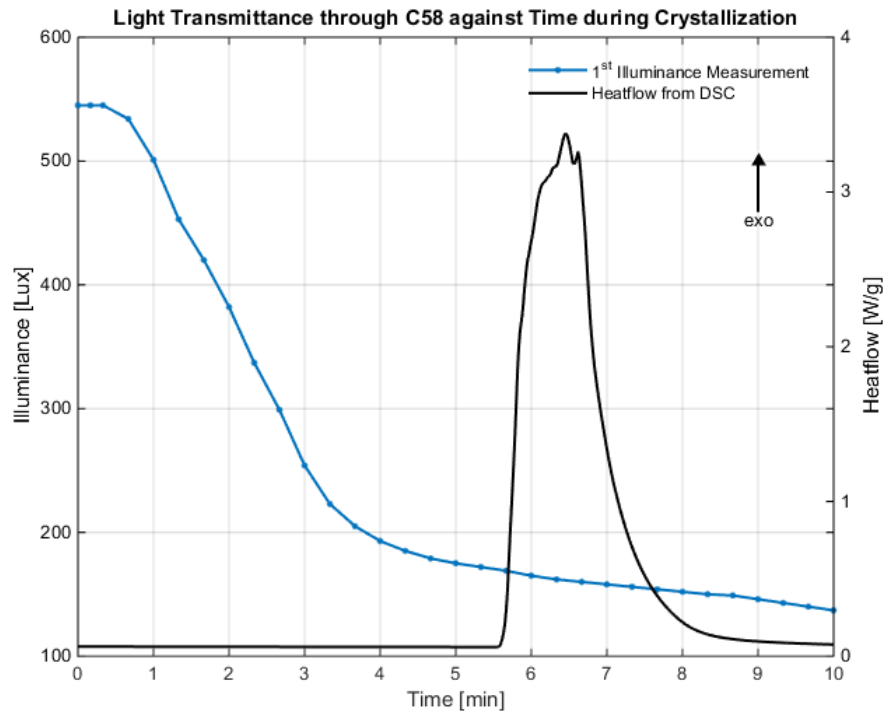


**Figure C-3:** *This figure shows a time plot for C58 from the light transmittance measurement and is a complement to figure 25.*
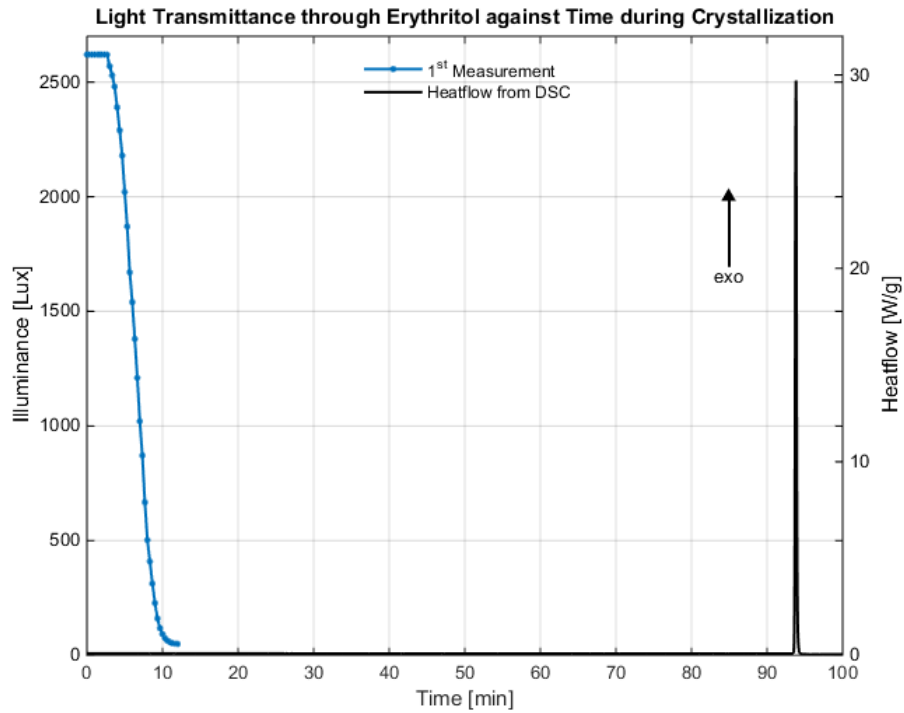
***Figure C-4:*** *This figure shows a time plot for erythritol from the light transmittance measurement and is a complement to figure 24.*
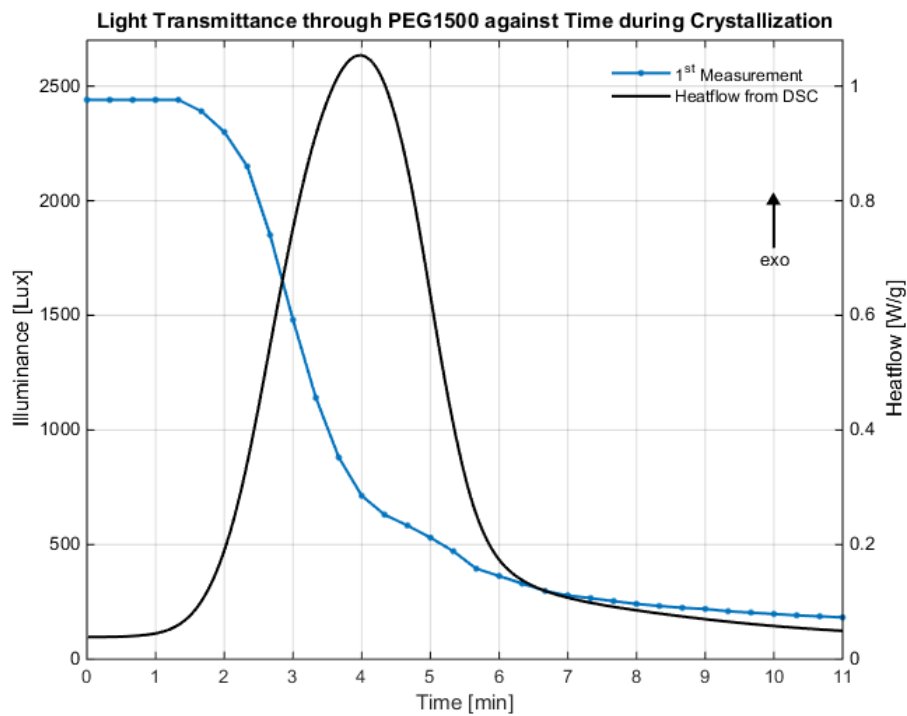


***Figure C-5:*** *This figure shows a time plot for PEG1500 from the light transmittance measurement and is a complement to figure 23.*
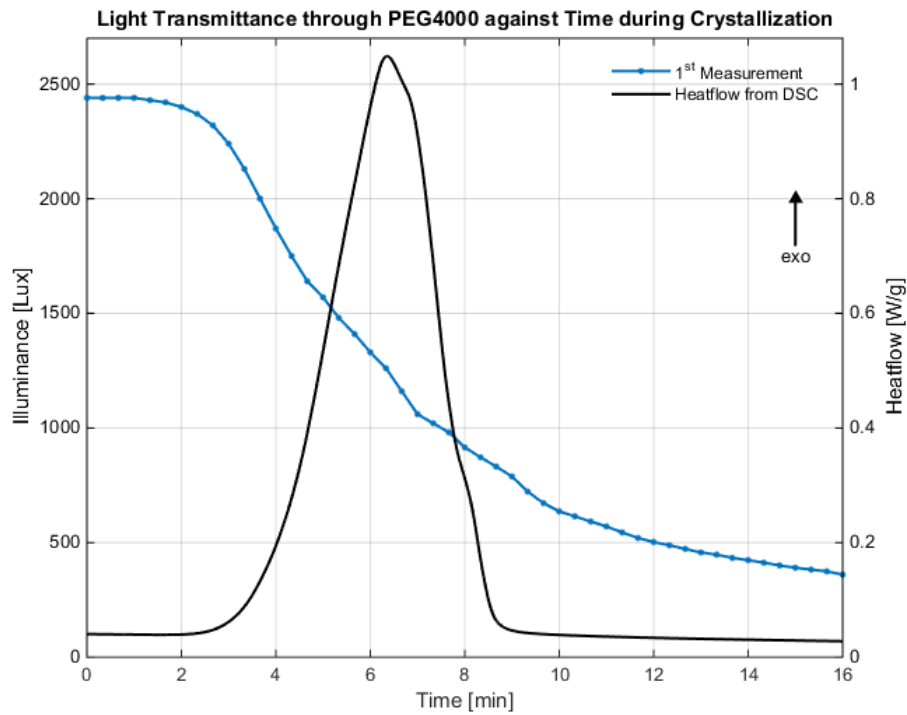
***Figure C-6:*** *This figure shows a time plot for PEG4000 from the light transmittance measurement and is a complement to figure c-1.*
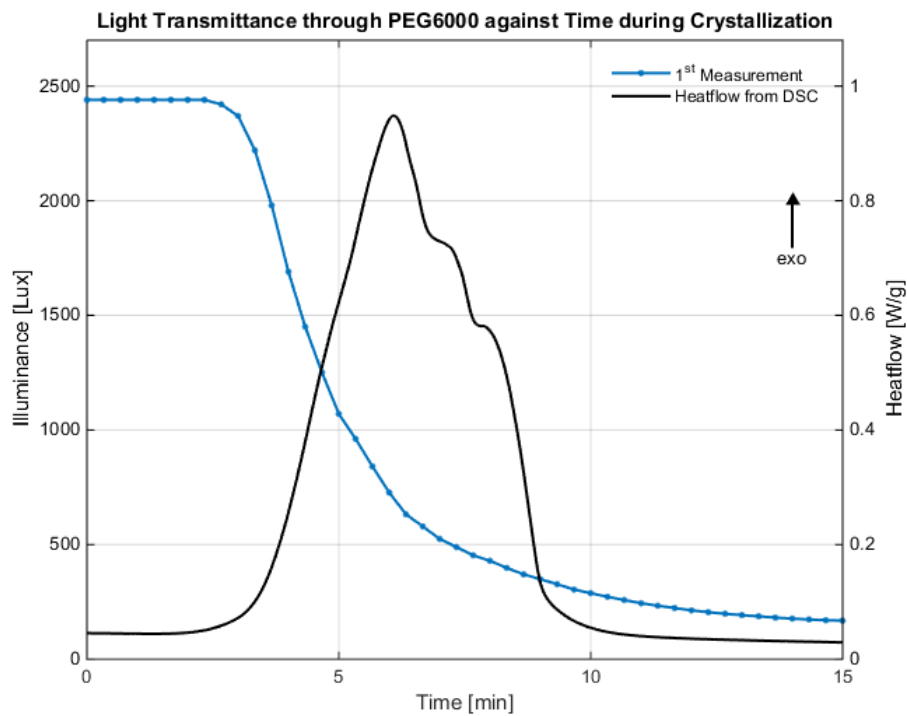


***Figure C-7:*** *This figure shows a time plot for PEG6000 from the light transmittance measurement and is a complement to figure c-2.*

# Appendix D. Complementary Results to Electrical Resistance Measurements

This appendix contains results from the electrical resistance measurements for xylitol as well as complementary time plots for erythritol and PEG1500. The results were obtained using the same method as described in section 4.2.5.
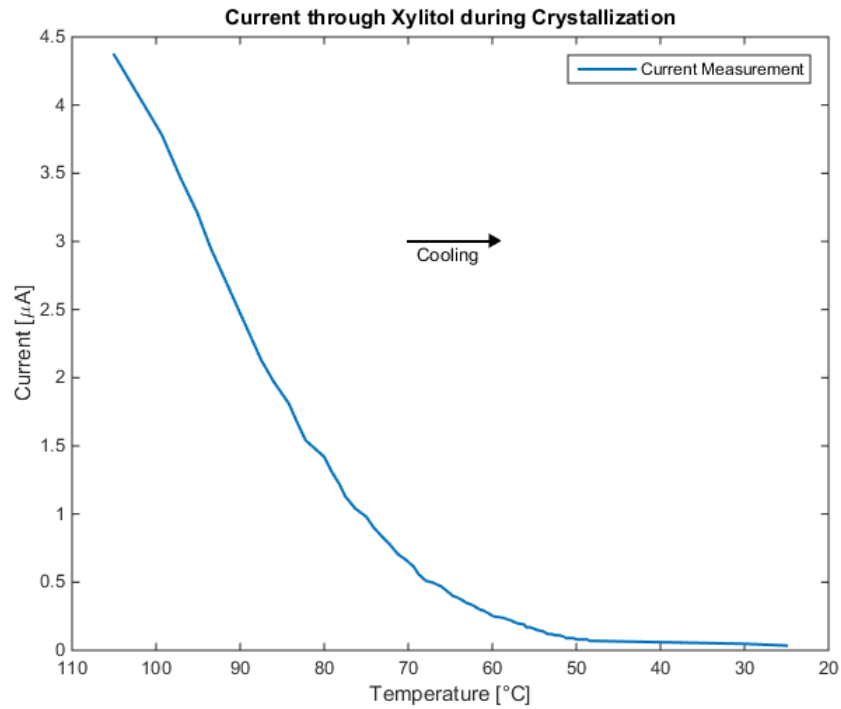


***Figure D- 1:*** *This figure shows the electrical resistance measurements for xylitol without DSC reference.*
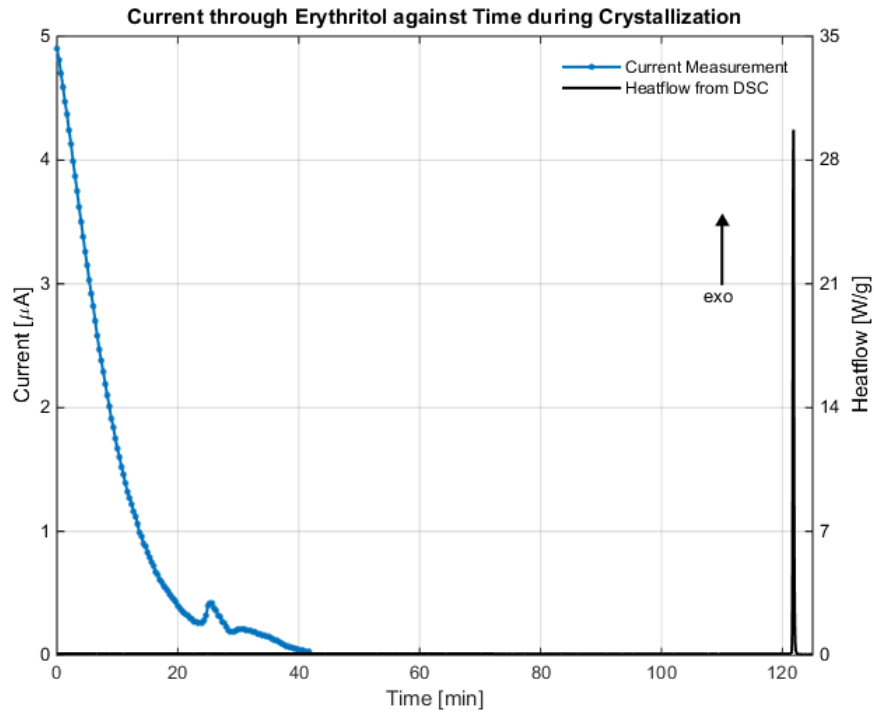
***Figure D-2:*** *This figure shows a time plot for erythritol from the electrical resistance measurement and is a complement to figure 28.*
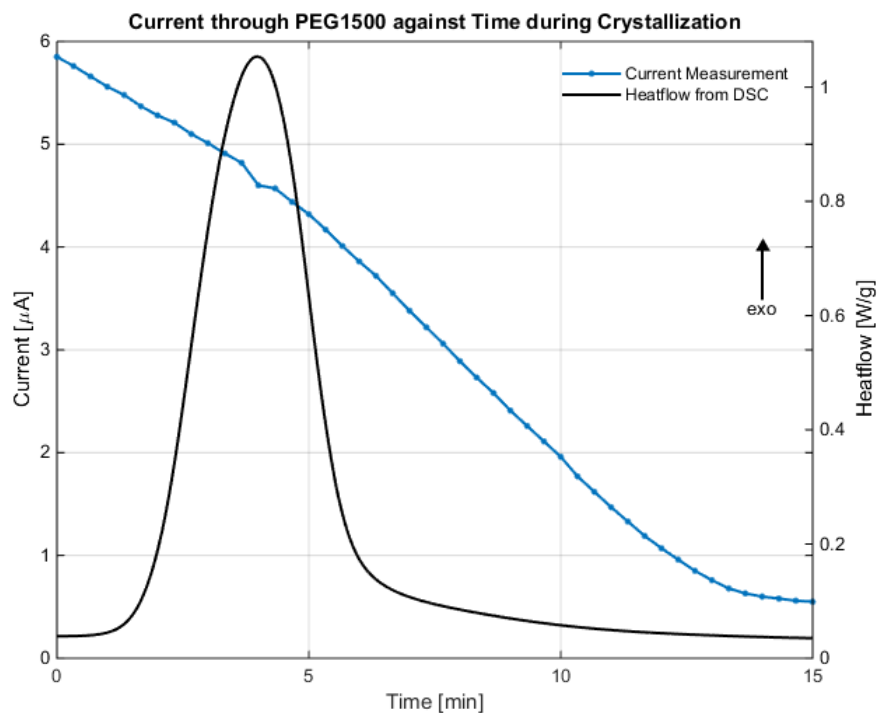


***Figure D-3:*** *This figure shows a time plot for PEG1500 from the electrical resistance measurement and is a complement to figure 27.*

# Appendix E.    Complementary Results to Dielectric Measurements

This appendix contains the results from the dielectric measurements for PEG1000 and erythritol with artifacts still present. The results were obtained following the same procedure as described in section 4.2.6.
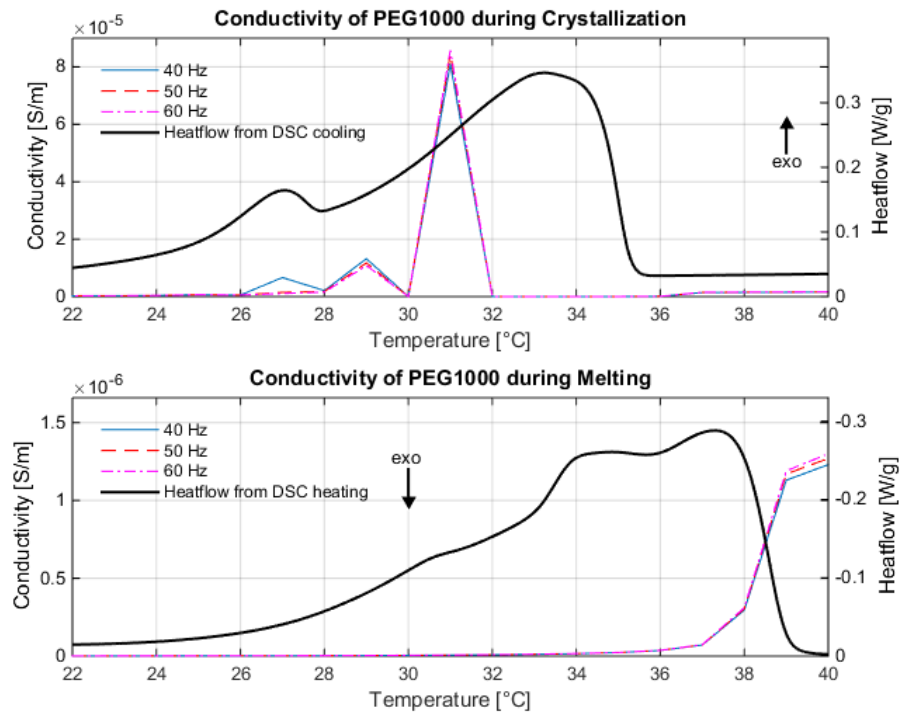


***Figure E-1:*** *This figure shows the results from conductivity measurement for PEG1000 with artifacts.*
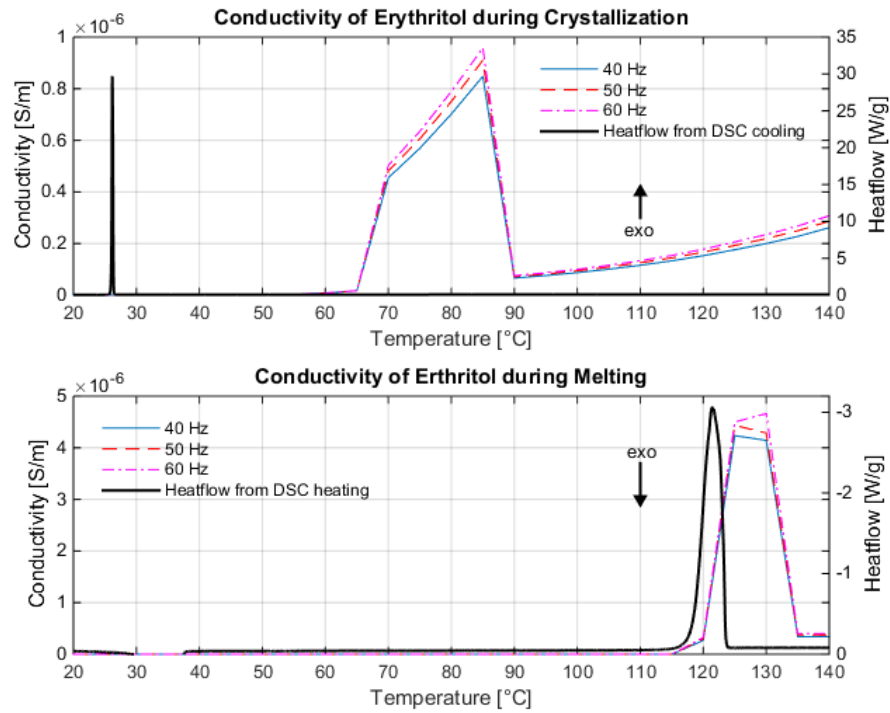
***Figure E- 2:*** *This figure shows the results from conductivity measurement for erythritol with artifacts.*